

Utah State University

DigitalCommons@USU

Undergraduate Honors Capstone Projects

Honors Program

5-1998

Research and Design of a High L/D Aircraft

Blake Ashby
Utah State University

Gregory Nielson
Utah State University

Follow this and additional works at: <https://digitalcommons.usu.edu/honors>

 Part of the [Aerospace Engineering Commons](#), and the [Mechanical Engineering Commons](#)

Recommended Citation

Ashby, Blake and Nielson, Gregory, "Research and Design of a High L/D Aircraft" (1998). *Undergraduate Honors Capstone Projects*. 948.

<https://digitalcommons.usu.edu/honors/948>

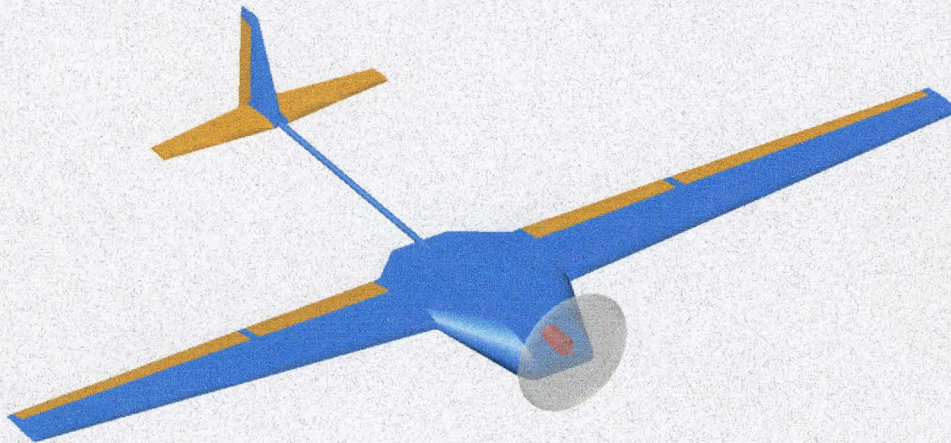
This Thesis is brought to you for free and open access by the Honors Program at DigitalCommons@USU. It has been accepted for inclusion in Undergraduate Honors Capstone Projects by an authorized administrator of DigitalCommons@USU. For more information, please contact digitalcommons@usu.edu.



1997-98 Mechanical & Aerospace Engineering Senior Design

Research and Design of a High L/D Aircraft

May 15, 1998



Airteam 2
Blake Ashby
Shelly Barlow
Greg Nielson
Deryl Snyder
Christopher Wright

RESEARCH AND DESIGN OF A HIGH L/D AIRCRAFT

By

Blake Ashby and Gregory Nielson

**Thesis submitted in partial fulfillment
of the requirements for the degree**

of

DEPARTMENT HONORS

in

Mechanical and Aerospace Engineering

Approved:

Thesis/Project Advisor

Department Honors Advisor

Director of Honors Program

**UTAH STATE UNIVERSITY
Logan, Utah**

1998

1997-98 Mechanical & Aerospace Engineering Senior Design

Research and Design of a High L/D Aircraft

May 15, 1998

Submitted to

Dr. J. Clair Batty
Department of Mechanical & Aerospace Engineering
Utah State University
Logan, UT 84322-4310

Submitted by

Airteam 2

Blake Ashby

Shelly Barlow

Greg Nielson

Deryl Snyder

Christopher Wright

Faculty Advisor

Warren F. Phillips

Table of Contents

Acknowledgements	1
Executive Summary	2
Introduction	4
Objectives	5
Requirements	5
Requirements Imposed by the Competition	5
Takeoff	5
Maneuverability	6
Landing	6
Power Plant	6
Payload	6
Structural Integrity	6
Safety	7
Requirements Imposed by Team Members	7
L/D ratio	7
Construction	7
Flight Speed	7
Handling	7
Weight	7
Conceptual Design	8
Alternative Concepts	8
Tail vs. Canard Configuration	8
High vs. Low Wing	9
Conventional Tail vs. V-tail	9
One-Motor vs. Two-Motors	9
Brushless vs. Brush Motor	9
Payload in Fuselage vs. Payload in Wing	9
Center of Gravity In Front Of vs. Behind Wing Quarter-Chord	10
Cylindrical Fuselage vs. Airfoil-Shaped Fuselage	10
Composite vs. Spruce Wood Beams in Wing	10
Landing Gear—Tail-Dragger vs. Nose-Wheel	10
Tapered vs. Rectangular Wing	11
Figures of Merit Summary	11
Preliminary Design	13
Analytical Methods and Tools	13
“Airplane” Program	13
“Params” Program	13
“Mpeff” Program	14
“Wind_DS” Program	15
“Analyse an Airfoil” Program	16
Design Parameter and Sizing Selection	16
Flight Speed	16

Reducing Planform Area _____	18
<i>Detail Design</i> _____	20
Final Performance Data _____	20
Takeoff Performance _____	20
Handling Qualities _____	21
Range and Endurance _____	24
G-load Capability _____	25
Payload Fraction _____	26
Wind Analysis _____	27
Other Performance Plots _____	29
Power Plant Component Selection _____	32
Drawing Package _____	34
<i>Manufacturing Plan</i> _____	34
Wing Construction _____	34
Beam _____	34
Foam Core _____	35
Balsa/Ultrakote Sheeting _____	36
Control Surfaces _____	36
Fuselage Construction _____	36
Frame _____	36
Access Hatch _____	37
Motor Mount _____	37
Beam to Tail _____	37
Landing Gear _____	37
Tail Construction _____	37
Cost of Designed Airplane _____	38
Manufacturing Milestone Chart _____	40
<i>Flight Testing</i> _____	40
Push Rods _____	40
Landing Gear _____	40
Power Plant _____	40
Wing Size _____	42
<i>Competition</i> _____	42
Design Report _____	42
Fly-Off _____	42
<i>Areas for Improvement in Next Design</i> _____	42
Tail Boom Design _____	42
Main Support Beam in Wing _____	43

Easy Modifications	43
Battery Pack	43
Control Surfaces	43
<i>References</i>	43
<i>Appendix A--Equations Relating to Power Plant</i>	44
<i>Appendix B—Takeoff Analysis</i>	46
<i>Appendix C—Detailed Drawing Package of Final Design</i>	48

Acknowledgements

We would like to thank the following for their help in making this senior design project a positive and successful learning experience.

Dr. Warren F. Phillips
Jim Fufarro
Dave Stewart
Dr. J.C. Batty
Gordon May
Terry Zollinger
Airteam3
Airteam1
AIAA
Cessna
Office of Naval Research (ONR)

Executive Summary

A design team at Utah State University designed, analyzed, and built an airplane that competed in the 1997/98 Cessna/ONR Student Design/Build/Fly Competition sponsored by AIAA in Wichita, Kansas on April 25, 1998. This design project was to develop an unmanned, electric-powered, radio-controlled airplane to complete the most laps around a specified course in a seven-minute time limit. The airplane was powered by 2.5 pounds of NiCad batteries and carried a 7.5 pound steel payload.

The conceptual design of the airplane began with making initial design decisions and weighing tradeoffs. One of the more significant aspects of the design was whether to build an airplane with a tail configuration or a canard configuration. The tail configuration was selected over the canard because of concerns about stability and construction. A cylindrical fuselage design was investigated as well as an airfoil-shaped fuselage. The airfoil-shaped fuselage was selected because it is lower in drag, lighter in weight, and less expensive to build. The composition of the structural beam for the wing support was also studied. Alternatives considered were box beams of spruce wood or carbon fiber composites. The composite beam was chosen because it provided the necessary strength and stiffness for the wing.

Numerous design tools and analytical methods were used at each step of the design process. Most of these methods involved the use of computer programs that were either already available or were developed by the team members. The first program used is the "Airplane" program, an aircraft design package developed at Utah State University. This program was used to iteratively modify the various parameters of the airplane at each step in the design process. The second program, "Params", was used throughout the design process to help evaluate the effects various design changes had upon the airplane's performance including lift-to-drag ratio, thrust available and required, power available and required, minimum turning radius, rate of climb, throttle setting required, and energy consumption. The third program, "Mpeff" (for Motor/Propeller efficiency), was used in the selection of appropriate combinations for the electric motor, speed control, battery pack, and propeller. The fourth program, "Wind_DS", was developed by the design team to determine the effects of wind on the airplane's performance. The final program, "Analyse an Airfoil", was used to help the design team select a suitable airfoil shape for the wing.

One of the most important decisions made was the designed airspeed of the airplane. Initially, the airplane was designed to fly at 30 mph. It was determined that the time would expire much sooner than the available battery power at this airspeed. Therefore, the planform area of the airplane needed to be significantly decreased in order to increase the designed airspeed. Ideally, the team would have liked to design the airplane with a minimum drag airspeed of approximately 70 mph. However, structural limitations imposed by the need to carry the 7.5 pound payload made this task nearly impossible. Ultimately, the airplane was designed with a minimum drag airspeed of 53 mph, but will actually fly closer to 70 mph in order to use the available energy in the time allotted.

The structural design of the airplane made use of carbon fiber composite material for the structural members with Styrofoam sheeted with balsa wood and Ultrakote to give the airplane the proper shape. The driving factors in the structural design were ease of construction, material cost, and performance.

The flight testing of the airplane revealed several problems. The main problem encountered during the flight testing was inadequate power for takeoff with the payload. This problem was solved by purchasing a more powerful motor and increasing the size of the wings.

The design report submitted to the competition received the high score. However, the windy flight conditions at the contest prevented all but four planes from completing a qualifying flight. Utah State's airplane crashed on both flight attempts and therefore took fifth place behind the four qualifying teams.

Introduction

This senior design team, consisting of Blake Ashby, Shelly Barlow, Greg Nielson, Deryl Snyder, and Chris Wright, designed, built, and flew an airplane that met the requirements of the Cessna/ONR Student Design/Build/Fly Competition sponsored by AIAA. This radio-controlled airplane was designed to fly the most laps around a course in seven minutes using only 2.5 pounds of NiCad batteries. A total of three senior design teams from Utah State University designed separate airplanes. Though all three teams designed, built, and tested complete airplanes, each emphasized a different aspect of a successful entry. This team emphasized theoretical and numerical analysis in order to build an aerodynamically clean and efficient airplane. The other teams stressed motor/propeller efficiency and electronic speed control. This team's airplane represented the university at the contest in Wichita, Kansas on April 25, 1998.

Four of the five students on this design team have taken two quarters of aerodynamics classes that provided them with a solid theoretical background in aircraft performance analysis and design. Designing and constructing a plane for this competition provided a real-world aircraft design experience that solidified and built upon classroom analytical training. The fifth student has solid experience and abilities in the areas of structural analysis and mechanics of composite materials.

This design problem was an ideal project for Senior Design for a number of reasons. First, the project allowed the students to apply engineering principles learned in the classroom in a tangible manner. This project required the application of engineering principles relating to statics, dynamics, electronics, manufacturing processes, fluid mechanics, aerodynamics, numerical methods, computer-aided drafting, mechanics of materials (including composites), finite-element analysis, and control systems. In addition, since this airplane was actually built, so the participating students were able to see the entire design process from start to finish. As a result, the team was forced to design for manufacturability. Each student in the group has his or her own strengths, and this experience allowed each group member to contribute in a significant way to accomplishing the team's objectives. The workload breakdown of the team is summarized in Table 1 where '5' indicates maximum involvement.

Table 1--Team Involvement

Task	Blake Ashby	Deryl Snyder	Shelly Barlow	Greg Nielson	Chris Wright
Conceptual Design					
Basic Airplane Configuration	5	5	5	0	5
Construction Techniques	2	2	5	5	5
Preliminary Design					
Software Development	3	5	0	0	0
Aerodynamic Analysis	5	5	2	0	2
Structural Analysis	0	0	2	5	5
Structural Testing	0	2	5	5	5
Detail Design					
Aerodynamic Analysis	5	5	0	0	0
Power-Plant Configuration	5	2	0	0	0
Structural Design	0	3	3	5	5
Control Surface Sizing	2	0	5	0	0
Post-Design Phase					
Airplane Construction	2	3	5	3	5
Engineering Drawings	1	5	2	0	0
Design Report	5	5	0	2	0

Objectives

The ultimate objective for this senior design team was to design and build a plane to win the 1997-98 Cessna/ONR Student Design/Build/Fly Competition. The airplane needed to be designed to fly the most laps possible around a designated course within a seven-minute time period and land within the 300 foot marked runway. The team also had to submit a Design Report to the competition that details the design and analysis process performed by the team. Both the report and the airplane's performance at the competition were factors in determining the winning team. The team's ranking was determined by the following formula:

$$\text{Ranking} = (\text{Report Score}) * (\text{Laps} + \text{Landing})$$

A maximum of 100 points was possible for the report. One point was awarded for each lap completed and one point for a successful landing.

Requirements

Most of the requirements for this Senior Design project were detailed by the 1997/98 AIAA Student Design/Build/Fly Contest Rules. In addition, this senior design team set certain requirements for the design that exceeded the minimum specified by the contest.

Requirements Imposed by the Competition

In order to qualify for the competition, an unmanned, electric-powered, radio-controlled aircraft had to be designed and built to meet a number of criteria.

Takeoff

The airplane had to be able to take off unassisted and clear a six-foot obstacle within a marked 300 foot runway.

Maneuverability

During the backstretch of the first lap, the plane needed to complete 360 degree right-hand and left-hand turns as shown in Figure 1.

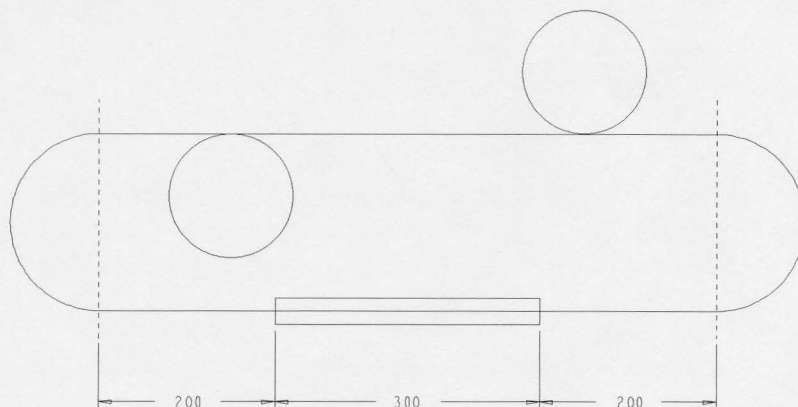


Figure 1--Course Layout

Landing

Once the first lap was completed, the airplane needed to complete at least one more lap to qualify. After completing as many laps as possible within seven minutes, the airplane needed to return and land within the original marked 300 foot runway. The aircraft did not need to come to a complete stop in this distance, but if it rolled out of the 300 foot area, it had to remain on the runway until coming to a complete stop without “bouncing.”

Power Plant

There were no imposed limits to the configuration of the airplane except that it could not be rotary wing or lighter-than air. The plane had to be propeller driven with one or more unmodified, over the counter model airplane motors. The motors could be direct, belt, or gear driven. The motors were to be powered by no more than 2.5 pounds of over the counter NiCad batteries. The individual battery cells needed to be commercially available, but the team could assemble these cells into a battery pack or buy a pre-assembled battery pack. The propeller also had to be commercially produced, but the diameter could be modified by clipping the tips.

Payload

The payload for the aircraft was 7.5 pounds of rectangular shaped steel that could be segmented into no more than three sections. The team had to be able to remove the payload within ten minutes. In addition, the plane had to be able to demonstrate acceptable handling and center of gravity location by completing two laps without the steel payload.

Structural Integrity

The airplane needed to be designed with adequate structural integrity as well. Sufficient wing strength was demonstrated at the competition by maintaining structural integrity when the loaded aircraft is lifted off the ground by the wing tips, which is equivalent to a 2.5 g load case. For an officially scored flight, the aircraft had to be sturdy enough to avoid any damage that would prevent it from making a second flight. The only exception to this rule was the team could replace a damaged propeller between flights to make it flyable. Also, no components could fall from the aircraft during the flight.

Safety

The aircraft radio had to have a fail-safe mode that was automatically selected if the transmitter signal was lost. During-fail safe the aircraft receiver had to select:

- Throttle closed
- Full up elevator
- Full left aileron
- Full flaps down

Additionally, the aircraft needed to have a mechanical motor arming system separate from the onboard radio power switch. This could be a mechanical switch rated for the maximum current draw accessible from outside the aircraft, or could be a removable link such as an automotive 'blade' style fuse.

Requirements Imposed by Team Members

In addition to the requirements given by the contest authorities, this senior design team defined requirements that this airplane design had to meet.

L/D ratio

This team's emphasis was aerodynamic efficiency, so the lift-to-drag ratio was optimized for the altitude of Wichita, Kansas which is 1300 feet above sea level. This L/D requirement was initially set at 25.

Construction

Designing a plane that is relatively simple to manufacture was equally important. If the team cannot easily construct the aircraft, it does not matter how efficient the aircraft is on paper or on the computer. Once the airplane was constructed, the team performed numerous tests to compare the actual performance characteristics versus those predicted. The airplane had to be designed for easy modification in order to apply what was learned from the test flights. The airplane also needed to be easily transportable since the contest was in Wichita, Kansas.

Flight Speed

For a given airplane design, there exists an optimum velocity that maximizes L/D and minimizes energy consumption. Therefore, an initial requirement for this design was to ensure that the airplane flies at this minimum drag airspeed so that the available battery power is used most effectively. This design airspeed needed to be low enough to allow for ease of landing and a small turning radius, but high enough to achieve a high power plant efficiency and complete the maximum possible number of laps in less than seven minutes.

Handling

Another necessary objective was to build a plane that is easy for the pilot to fly. Good handling characteristics can be ensured by designing the plane with sufficient pitch, roll, and yaw stability. The degree of pitch stability is measured by the static margin, which must be greater than 10 percent. The slope of the rolling moment must be between -0.001 and -0.002, and the slope of the yawing moment must be greater than 0.0015.

Weight

While maintaining sufficient strength and integrity, the weight of the plane needed to be minimized. The team initially indicated the weight could not exceed 17 pounds including the 2.5 pounds of batteries and 7.5 pounds of steel payload.

Conceptual Design

A number of alternative concepts were investigated in the conceptual design process. The various design tradeoffs are discussed and evaluated below based on numerous design criteria or figures of merit. These include a high lift-to-drag (L/D) ratio, proper stability, maneuverability, sufficient power, high power-plant efficiencies, cost, ease of construction, weight, team members' experience, strength, and wing deflection.

Alternative Concepts

Tail vs. Canard Configuration

One of the first design decisions made was whether to build an airplane with a traditional wing/tail configuration or with a canard/wing configuration. Designs for both configurations were developed on the computer using the "Airplane" program developed at Utah State University (see Figure 2 and Figure 3). Initially, it appeared that the canard configuration could achieve a slightly higher L/D. However, in order to achieve this, significant sweep was placed in the wings to keep the center of gravity closer to the main wings. The center of gravity needed to be located near the wings because the airplane had to be lifted from its wing tips at the competition. A swept wing introduces greater challenges in construction than a non-swept wing. Moreover, team members felt more comfortable designing and building a traditional wing/tail configuration than a canard configuration. Overall, the need to easily achieve proper stability, center of gravity location, and ease of manufacture outweighed the slight advantage in L/D ratio causing the team to select the wing/tail configuration.

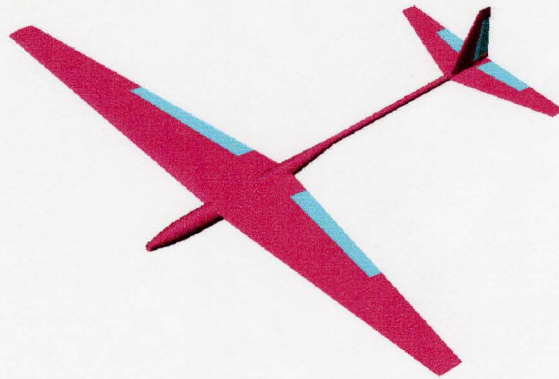


Figure 2--Conceptual Tail Configuration

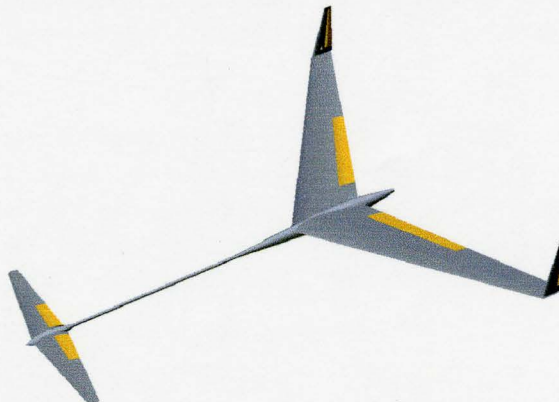


Figure 3--Conceptual Canard Configuration

High vs. Low Wing

The team investigated the advantages and disadvantages of a design with a high wing versus a low wing. In terms of performance (L/D), there was no perceived benefit of one configuration over the other. However, the high wing design makes it easier to achieve sufficient roll stability and therefore requires that less dihedral be designed into the wing. The reason for this is that the airflow around the fuselage creates a stabilizing roll moment for a high wing and a destabilizing roll moment for a low wing. A wing with less dihedral is a more efficient lifting surface because the lifting force vector is closer to vertical. Also, a low-dihedral wing simplifies construction. Therefore, the team decided to design for a high wing configuration.

Conventional Tail vs. V-tail

Some consideration was given to using a V-type tail in place of the conventional horizontal and vertical tail surfaces. The justification for this was to reduce drag because there would only be two surfaces instead of three (left and right horizontal tail and vertical tail). This type of configuration introduces other complications in ensuring stability, the design of control surfaces, and construction. The team members felt more comfortable with the conventional configuration and the reduction in drag by the V-tail was not significant, so the conventional tail was selected.

One-Motor vs. Two-Motors

Higher power-plant efficiencies in steady-level flight is the justification for using two motors instead of one. Motors run more efficiently at higher throttle settings. However, a design that requires the motor operate near full throttle just to sustain steady-level flight would not have enough power to lift-off in the required 300 feet runway. Therefore, a more powerful motor could be used to takeoff, and once the desired altitude is achieved, the power could be switched to a second motor which is more efficient at the flying speed. This setup would use the available battery power more efficiently. However, this type of setup is significantly more complicated to design and build. Also, the cost and weight needed for the motors would be twice as much. The design team determined that the small increase in efficiency did not outweigh the extra cost, weight, and design difficulty necessary to implement it, so the single motor system was selected.

Brushless vs. Brush Motor

Another significant decision in this design process was whether to use a brushless or a brush motor for propulsion. Brushless motors generally perform more efficiently than brush motors. Brushless motors have lower internal resistance and lower frictional losses than brush motors and therefore run cooler at higher currents. Cooler running motors are more efficient because the resistance of the copper in the motors increases with temperature. Another positive attribute of brushless motors according to the manufacturer is that there is less radio noise generated that can interfere with the remote control. In addition, the weight of the brushless motor selected for our design is slightly less than the brush motor that meets our design requirements.

The main drawback to the brushless motor systems is they cost significantly more than a suitable brush motor system. Also, the lack of experience with the new brushless motors caused the team to question how reliable they are compared with the brush motors that have been used for years. Although the brushless motors perform more efficiently, the team initially felt they could not justify the extra expense for one extra lap (see Figure 17 and Figure 18). Therefore, the brush motor system was selected at this stage.

Payload in Fuselage vs. Payload in Wing

Another consideration investigated was where to place the 7.5 pound steel payload. An alternative to placing the steel in the fuselage is placing the steel inside the wing. The main benefit of this is the load from the steel would no longer be concentrated at the center of the wing, but would be distributed over a wider area, decreasing the necessary strength of the beam in the wing. One drawback to this design is that the

steel in the wings would increase the rolling moment of inertia of the airplane. This would require the ailerons be made larger in order effectively control the airplane. Calculations about how far the steel would need to extend from the fuselage into the wing were made assuming the steel would be placed inside the tapered box beams that run the length of the wing. As the wing area was decreased as discussed in the Preliminary Design section, placing the payload inside the tapered box beams became less and less feasible. Therefore, the design team finally elected to place the payload in the fuselage.

Center of Gravity In Front Of vs. Behind Wing Quarter-Chord

A plane with the center of gravity ahead of the quarter-chord of the wing will always be stable in pitch. In general, the horizontal tail generates negative lift to balance the airplane in flight. If the center of gravity is ahead of the quarter-chord of the main wing, the horizontal tail must generate more negative lift than if the center of gravity is behind the quarter-chord. Therefore, an airplane with the center of gravity located further back will have a higher overall lift-to-drag ratio. Ensuring pitch stability with this configuration is only slightly more difficult. Since it is easy enough to design a stable airplane with the center of gravity behind the quarter-chord of the main wing, the design team decided to do so in order to increase the L/D ratio of the airplane.

Cylindrical Fuselage vs. Airfoil-Shaped Fuselage

The two main fuselage configurations considered are the cylindrical fuselage and the airfoil-shaped fuselage. The cylindrical fuselage design is more conventional and therefore easier to design and adds more flexibility to the location of the internal components. The second approach investigated was an innovative airfoil wing/fuselage design. In this design, the fuselage would simply be an enlargement in the center of the wing and would still maintain an airfoil shape (though non-cambered). The fuselage would be constructed just like the wing with a foam core surrounded by a balsa and Ultrakote sheeting. Hatches would be constructed in the top of the fuselage and the various components would be attached inside of the Styrofoam. This design is a little more complicated to develop, but it provides great benefits in terms of reduced drag, weight, and cost over the cylindrical fuselage design.

Composite vs. Spruce Wood Beams in Wing

The conceptual design of the wing required a beam structural member in the wing. Several different beams were analyzed including beams composed of aluminum, various kinds of wood, and composite fiber materials. These beams were analyzed with a variety of cross-sectional shapes from circular and square solid beams to I-beams and box beams. These beams went through an initial screening based on weight, deflection, and ultimate strength. The aluminum beams were eliminated because of weight.

The beams that looked promising were a box beam that had a very thin airplane modelers plywood as a webbing that held either spruce or carbon fiber composite spars as far as possible away from the neutral axis. Both beam designs were constructed and tested. The spruce beam had a slightly lower weight but a greater deflection and lower ultimate strength than the carbon fiber beam. A large deflection in the main beam would transfer a large portion of the load to the foam core and balsa sheeting of the wing. Since the foam core and balsa sheeting of the wing itself can not support the deflection generated with the spruce beam, the carbon fiber composite beam was selected despite its slightly larger weight.

Landing Gear—Tail-Dragger vs. Nose-Wheel

The two concepts investigated concerning the landing gear were the “tail-dragger” and “nose-wheel” configurations. The “nose-wheel” configuration consists of the traditional two wheel landing gear located behind the center of gravity and a wheel placed towards the nose of the plane. The “tail-dragger” has the same two-wheel landing gear placed in front of the center of gravity with a small wheel attached to the rudder. The “tail-dragger” setup requires less weight and develops less drag in flight than the “nose-wheel”

configuration. Also, construction of the “tail-dragger” is less complicated because steering is achieved by simply attaching the tail-wheel to the rudder, requiring no additional servo linkages. Therefore, the “tail-dragger landing gear was chosen.

In addition, the possibility of using retractable landing gear to reduce the drag in flight was investigated. However, the design team decided against using retractable landing gear, because they would add significant weight and cost to the final design.

Tapered vs. Rectangular Wing

A tapered wing provides benefits in terms of aerodynamic efficiency over a rectangular shaped wing. Also, for a given wing area, a tapered wing allows for a larger root chord. This is important because the maximum moment occurs at the root and that is where the maximum strength must be. However, too much taper makes the wing tips small which increases the probability of wing tip stall. A rectangular wing is easier to build, but less efficient. All things considered, the team decided to design for a tapered wing. The specifics regarding the team’s selection of the taper ratio are detailed in the Preliminary Design section.

Figures of Merit Summary

Table 1 gives subjective quantitative values for each of the figures of merit for competing concepts. Each figure of merit was rated from ‘1’ to ‘3’ with ‘3’ being best. Values of ‘0’ were given when the figure of merit did not apply. The chosen design concept is shown in bold.

Table 2--Final Ranking Chart for Alternative Concepts

	High L/D	Stability/Maneuverability	Sufficient Power	Power-plant efficiency	Cost	Manufacturability	Weight	Team Experience	Strength	Deflection	Total Score
Wing/Tail	2	2	0	0	0	3	0	3	0	0	10
Canard/Wing	3	1	0	0	0	1	0	1	0	0	6
High Wing	1	3	0	0	0	2	0	0	0	0	6
Low Wing	0	1	0	0	0	1	0	0	0	0	2
V-Tail	2	0	0	0	0	1	0	1	0	0	4
Conventional Tail	1	0	0	0	0	2	0	2	0	0	5
1 motor	0	0	2	2	3	3	2	3	0	0	15
2 motors	0	0	3	3	1	1	1	1	0	0	10
Brushless motor	0	0	3	3	1	0	2	1	0	0	10
Brush motor	0	0	2	2	2	0	1	3	0	0	10
Steel in wings	0	1	0	0	0	1	0	1	0	0	3
Steel in fuselage	0	2	0	0	0	3	0	2	0	0	7
CG behind 1/4-chord	3	1	0	0	0	0	0	0	0	0	4
CG in front of 1/4-chord	1	2	0	0	0	0	0	0	0	0	3
Cylindrical Fuselage	1	0	0	0	1	2	1	0	0	0	5
Airfoil-shaped fuselage	2	0	0	0	2	1	2	0	0	0	7
Composite wing beam	0	0	0	0	1	1	2	2	3	3	12
Spruce wing beam	0	0	0	0	2	2	3	2	1	1	11
Tail-Dragger	2	1	0	0	0	2	2	0	0	0	7
Nose-Wheel	1	2	0	0	0	1	1	0	0	0	5
Tapered Wing	3	0	0	0	0	1	0	0	2	2	8
Rectangular Wing	2	0	0	0	0	2	0	0	1	1	6

Preliminary Design

Analytical Methods and Tools

A number of analytical methods were used at each step of the design process. Most of these methods involved the use of computer programs that are detailed below.

“Airplane” Program

The “Airplane” program is an aircraft design software package developed at Utah State University. It uses Prandtl’s lifting line theory to predict the induced drag and the downwash of all the elements on each other. Boundary layer theory is used to predict the parasitic drag on all the components. “Airplane” also accesses another program called “Airfoil” that uses potential flow panel methods to determine the characteristics of the chosen airfoil for the lifting surfaces.

This program was used to iteratively modify the major parameters of the airplane design. At each step, the user can see how the design looks and study the aerodynamic and stability characteristics of the design. This program proved to be the major tool in sizing the various components and exploring various design tradeoffs. There are some limitations to this software that made it difficult to accurately model the design. For example, the program does not take into account landing gear and the fuselage can only be represented by circular, oval, or polygonal shapes.

“Params” Program

“Params” is a program developed by the design team to assist in the performance determination of the airplane at each step of the design process. “Params” uses data files of the lift and drag coefficients at varying angles of attack generated by the “Airplane” program. A C_L vs. C_D curve is generated and the constant coefficients C_{D0} , C_{DL0} , and e are calculated with a least squares fit for the following 2nd-order relation:

$$C_D = C_{D0} + C_{DL0}C_L + \frac{C_L^2}{\pi eAR} \quad (1)$$

where C_{D0} is the drag coefficient at zero lift, C_{DL0} is the drag slope at zero lift, and e , is the Oswald efficiency factor. These three coefficients effectively describe the lift versus drag characteristics of the airplane and are used throughout the programs “Params”, “Mpeff”, and “Wind” for the various analyses.

To account for the effects of the landing gear neglected by the “Airplane” program, a typical landing gear was tested in the wind tunnel at Utah State University. The drag coefficient was determined and added to the C_{D0} term for the analysis.

Numerous parameters can be studied as a function of airspeed for the particular airplane design with the many plots “Params” easily generates. The performance plots menu from “Params” is shown in Figure 4. Some specific plots for the final airplane design are included in the Detail Design section.

In addition, given the appropriate motor, speed control, propeller, and battery pack parameters, “Params” performs a detailed take-off analysis using a fourth-order Runge-Kutta method. The final and maybe most important analysis “Params” performs uses information from the energy consumption, minimum turning radius, and take-off analyses to generate a plot of the maximum number of laps the airplane can complete as a function of airspeed.

Performance Plot Options:

0. Return to Main Options
 1. Lift-to-drag ratio
 2. Thrust Required
 3. Power Required
 4. Minimum turning radius
 5. Motor/prop efficiency (at thrust required for airspeed)
 6. Thrust available (different air densities)
 7. Thrust available (different throttle settings)
 8. Thrust available with thrust required (different throttle settings)
 9. Power available (different air densities)
 10. Power available (different throttle settings)
 11. Power available with power required (different throttle settings)
 12. Rate of climb (different air densities)
 13. Rate of climb (different throttle settings)
 14. Throttle setting required for steady, level flight
 15. Energy consumption rate at steady level flight
 16. Energy consumed per lap using minimum turning radius
 17. Energy consumed per lap (varying turning radii)
- >

Figure 4 -- Performance Plots menu of "Params" program.

"Mpeff" Program

A detailed analysis of the power plant of the airplane was performed in order to select appropriate combinations for the electric motor, speed controller, battery pack, and propeller. "Mpeff", a program developed by the design team, was used extensively in this process. This program uses equations relating the various components derived from the simple schematic shown in Figure 5.

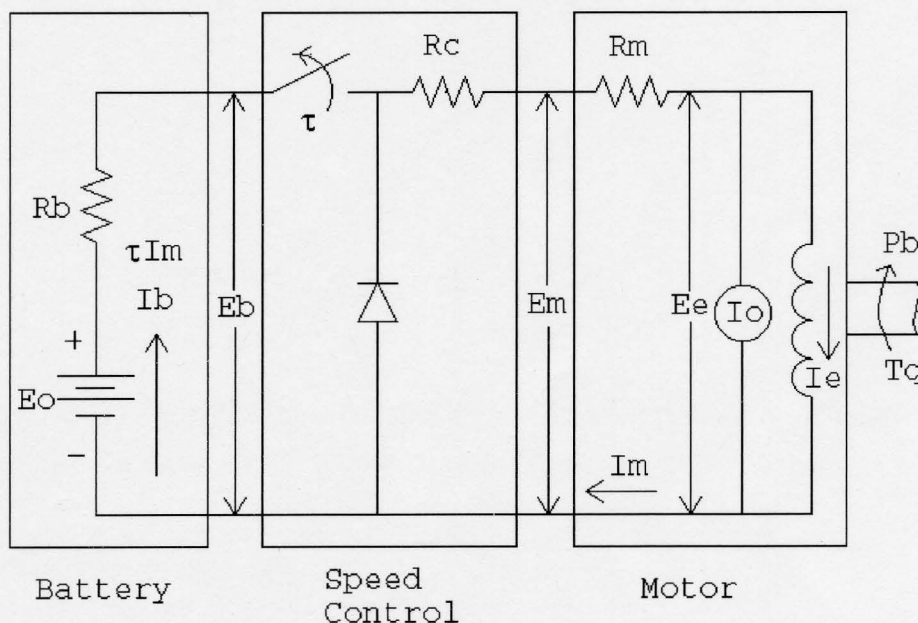


Figure 5--Schematic of Motor/Speed Control/Battery System

The power required to turn the propeller shaft and the thrust delivered by the propeller were calculated according to equations developed from limited empirical data gathered from *Electric Motor Handbook* written by Robert J. Boucher of Astroflight, Inc. These equations relate the propeller performance to its pitch and diameter. All the equations that “Mpeff” uses to describe this model are detailed in Appendix A.

“Wind_DS” Program

The “Wind_DS” program was developed to determine the effects of a head wind, crosswind, or tail wind on the airplane’s performance. This software calculates the optimum constant airspeed for the entire course as a function of wind direction and speed.

The first step in developing the model was to relate the ground speed to the airspeed and wind speed and direction; Figure 6 shows this relation. From the figure, it is seen that if the aircraft is flying directly into a headwind, the ground speed will be less than the airspeed by an amount equal to the speed of the wind. If the aircraft is flying directly with a tailwind, the ground speed will be equal to the sum of the airspeed and the wind speed. A crosswind also effects the ground speed of the aircraft because in order to maintain a specified ground track over the ground, the pilot must “crab” into the wind at an angle to the desired line of flight. When flying in a direct crosswind, only one component of the airspeed contributes to the ground speed, the other must balance the crosswind to keep the aircraft from drifting off track.

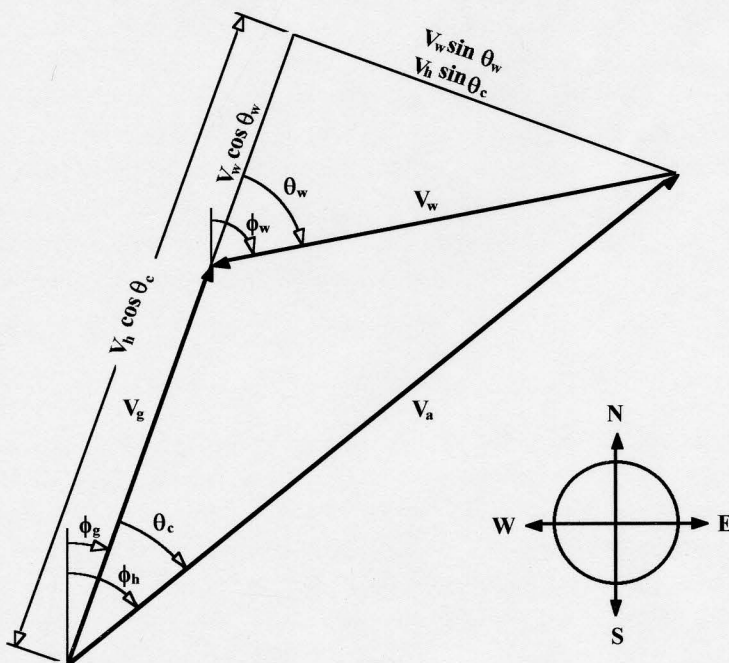


Figure 6 -- The relationship between ground speed, airspeed, and wind speed

Using Figure 6, it can be shown that the ground speed, V_g , is given as

$$V_g = \sqrt{V_a^2 - V_{cw}^2} - V_{hw} \quad (2)$$

where V_a is the airspeed, V_{cw} is the crosswind component, and V_{hw} is the headwind component.

While the aircraft is in a turn, the wind will cause the entire "turning curve" to move. The amount that this curve is shifted, X_{hw} or X_{cw} , is simply the wind speed multiplied by the time in the turn, or

$$X_{hw} = \left(\frac{\pi R}{V_a} \right) \cdot V_{hw} \quad X_{cw} = \left(\frac{\pi R}{V_a} \right) \cdot V_{cw} \quad (3), (4)$$

where R is the turning radius.

Taking these relations and the course geometry into account, the total time to complete a lap as a function of airspeed, headwind speed, and crosswind speed can be expressed as

$$t = \left(\frac{2L_s}{V_a} \right) \left(\frac{V_a \sqrt{V_a^2 - V_{cw}^2}}{V_a^2 - V_{hw}^2 - V_{cw}^2} \right) + \left(\frac{2\pi R}{V_a} \right) \left(\frac{V_a^2 + V_{cw}^2 \sqrt{V_a^2 - V_{hw}^2}}{V_a^2 - V_{hw}^2 - V_{cw}^2} \right) \quad (5)$$

What is learned from this model is explained later in the Detail Design section of this report.

“Analyse an Airfoil” Program

The “Analyse an Airfoil” program was written by Martin Hepperle and posted on the Internet at <http://beadec1.ea.bs.dlr.de/Airfoils/calcfoil.htm>. This program uses a second-order vortex panel method to calculate the velocity profile of the airfoil and uses an integral boundary layer method to compute the drag over the airfoil. With this program, the characteristics of the chosen airfoil were studied to make sure it performs well at low Reynolds numbers (~400,000) and provides sufficient lift. Specifically, it calculates and plots the lift, drag, and quarter-chord moment coefficients as a function of angle of attack. From this, the lift slope, maximum lift coefficient and stall angle of the airfoil can be determined. This program was used to analyze some common airfoils and the results corresponded very well with the experimental data published in *Theory of Wing Sections* by Abbott and Von Doenhoff.

Design Parameter and Sizing Selection

Flight Speed

One of the most critical decisions for this design was the selection of the best velocity to fly the airplane. Initially, it was decided to fly at a speed low enough to allow for ease of landing and small turning radii. Also, the airplane should fly fast enough to get good efficiencies with the power plant. Based only on intuition, the airplane was initially designed to fly at 30 mph. For a given airplane design, there is an optimum airspeed that maximizes the lift-to-drag ratio and minimizes the thrust required. This airspeed is referred to as the minimum drag airspeed, V_{MD} , or the best L/D airspeed. The V_{MD} and the drag at this airspeed can be closely approximated as follows:

$$V_{MD} = \frac{\sqrt{2}}{\sqrt[4]{\pi e AR C_{D0}}} \sqrt{\frac{W}{S}} \quad D_{min} = 2 \sqrt{\frac{C_{D0}}{\pi e AR}} W \quad (6), (7)$$

Equation (6) indicates that the terms that can be varied to adjust the minimum drag airspeed are the Oswald efficiency factor, e , the aspect ratio, AR , the weight, W , and the planform area, S . The air density, ρ , obviously cannot be controlled. V_{MD} can be increased by decreasing the Oswald efficiency factor and the aspect ratio. However, as is shown equation (7), decreasing those parameters would in turn increase the drag which is undesirable. Also, it is counterproductive to design an airplane for anything other than

minimum weight, so the only parameter that can really be adjusted to increase the minimum drag velocity is the wing planform area.

The effects of varying wing planform area and airspeed were studied to discover if there is an optimum planform area and airspeed for a given design. The results of this analysis are shown in Figure 7. This plot takes into consideration the course geometry, assuming the plane takes all turns at the minimum possible turning radius, and includes the variation of motor/prop efficiency with airspeed. From this plot, it is seen for a given planform area there is a corresponding optimal velocity which maximizes the number of possible laps. The shallow valley that becomes apparent at low planform areas is due to the transition between stall-limited and load-limited turns. Clearly, it is desirable to fly near the optimum airspeed to minimize the energy consumed per lap.

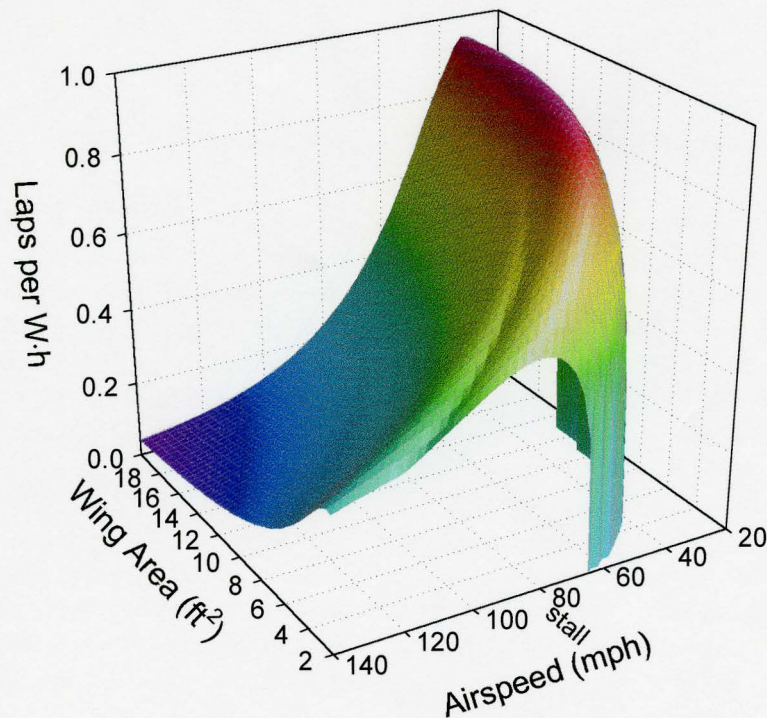


Figure 7--Number of Laps per W·h as a function of Airspeed and Planform Area

The next concern was how the seven-minute time limit affects the choice of airspeed. Using the energy consumption analysis capabilities of "Params", Figure 8 was generated. The airplane would clearly run out of time before it would run out of battery power if flown at 30 mph. The airplane needed to be designed to fly efficiently at a much higher airspeed. From the time limited curve it can be seen that, even if the airplane had infinite energy, there is a limit to the number of laps that could be completed in seven minutes. This maximum is due to the increasing minimum turning radius with increasing airspeed. At airspeeds above this maximum, any benefit of increased velocity is counteracted by an increase in distance around the course.

It can be seen from the plot that the airplane should fly at least 70 mph to complete the maximum number of laps in seven minutes. The planform area for the airplane designed to fly at 30 mph was about 11 ft². Thus, this value had to be reduced significantly to raise the minimum drag airspeed to an acceptable level and shift the energy limited curve to the right.

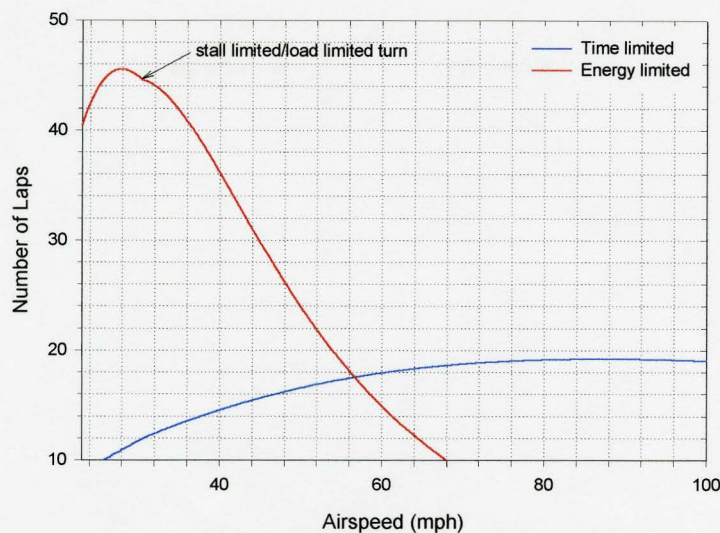


Figure 8--Maximum Number of Laps For Early Airplane Design

Reducing Planform Area

Many structural and manufacturing difficulties developed while reducing the wing area. To raise the minimum drag airspeed to 70 mph, the planform area would need to be reduced to approximately 1.85 ft². This is not realistic for a number of reasons. An airplane with that planform area that can lift a 7.5 pound payload would be difficult, if not impossible, to design and build. The smallest the design team felt comfortable with was a wing area of 3.0 ft². This corresponds to a V_{MD} of about 53 mph which is much closer to the desired flight speed of 70 mph.

Many design tradeoffs had to be made in reducing the planform area. The initial design called for an aspect ratio of about 18 which would increase the L/D ratio of the airplane. In order to keep this aspect ratio, the mean chord length of the wing needed to be reduced to 4.9 in. The design team felt that this was too small to manufacture the precise dimensions of the airfoil. Therefore, the minimum mean chord length was set at 6 in. This meant the aspect ratio of the main wing became 12.0 with a wing span of 6 feet. This resulted in some reductions in the L/D ratio, but not enough to decrease the airplane's predicted performance by even one lap.

Another parameter examined was the wing's taper ratio. According to calculations performed by the famous English aerodynamicist, Herman Gauert, a tapered wing is most efficient with a taper ratio of approximately 0.35 as shown in Figure 9 (Anderson). The lower the induced drag factor δ is, the more efficient the wing is. The initial design had a taper ratio of 0.35. However, maintaining this taper ratio required that the wing tip chord length be 3.1 in. Once again, the inability to manufacture a precise airfoil that small and the concern of wing tip stall in flight caused the design team to alter the taper ratio. A satisfactory compromise was achieved by setting the taper ratio at 0.5 which caused the wing tip chord length to be 4.0 in. and the wing root chord length to be 8.0 in. This taper ratio also provides structural benefits over an untapered wing by increasing the size of the root chord where the bending moment is maximum. Once again, the effects of this compromise were studied with the "Params" program, and still the airplane design's predicted number of laps did not decrease by going with a less efficient taper ratio.

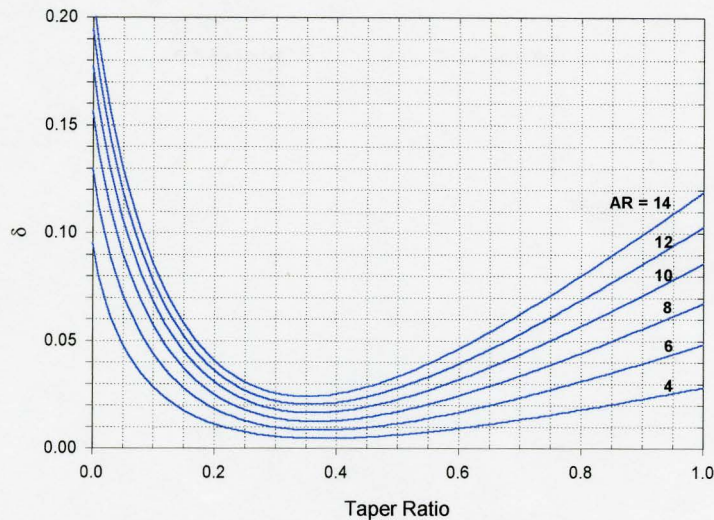


Figure 9--Induced Drag Factor δ vs. Taper Ratio

The location and size of the tail surfaces were determined using the “Airplane” program. The horizontal tail surface must be positioned and sized so that the airplane has no pitching moment about the center of gravity in flight. This moment is kept at zero by trimming the elevators in flight. In general, the further the tail is from the wing, the smaller it can be. The vertical tail surface was sized to be large enough to maintain yaw stability, but also as small as possible to reduce drag.

Finally, the airfoil was selected to provide the airplane with the proper performance characteristics. This design is a low Reynolds number application ($\sim 500,000$ at the wing root and $\sim 250,000$ at the wing tip) and therefore an airfoil that performs well at these Reynolds numbers was selected. The empirical data of the Wortman FX63B airfoil indicates good performance at low Reynolds numbers. However, the designed lift coefficient at zero angle of attack for this airfoil is approximately 1.17. This airplane design does not need such a heavily cambered airfoil, so this airfoil was modified using a program at Utah State University called “Airfoil”. The necessary lift coefficient at zero angle of attack to fly at 70 mph (103 ft/sec) and support the estimated weight of the airplane of 16 pounds was calculated with the following equation:

$$C_L = \frac{W}{\frac{1}{2} \rho V^2 S} = \frac{16lb}{\frac{1}{2} (0.002289 slug / ft^3) (103 ft / sec)^2 (3.0 ft)} = 0.44 \quad (8)$$

The thickness and camber distribution of the airfoil were maintained, and the maximum camber was altered so the designed lift coefficient at zero angle of attack was reduced to 0.52. This caused the lift coefficient of the whole airplane to be reduced to about 0.44 at zero angle of attack. A plot of the lift coefficient versus angle of attack is shown in Figure 10. This airfoil has a maximum lift coefficient of 1.53 with no flaps and 1.90 with 25% of the chord flaps deflected just 5 degrees. A plot of this airfoil is shown in Figure 11.

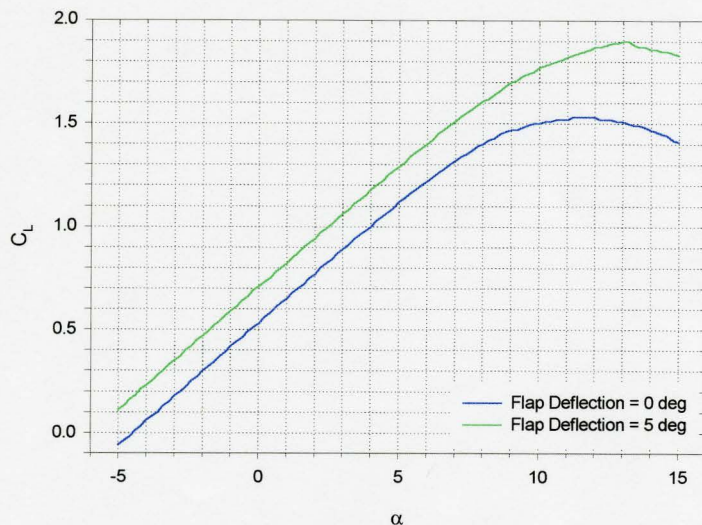


Figure 10-- C_L vs. Angle of Attack for Wing Airfoil

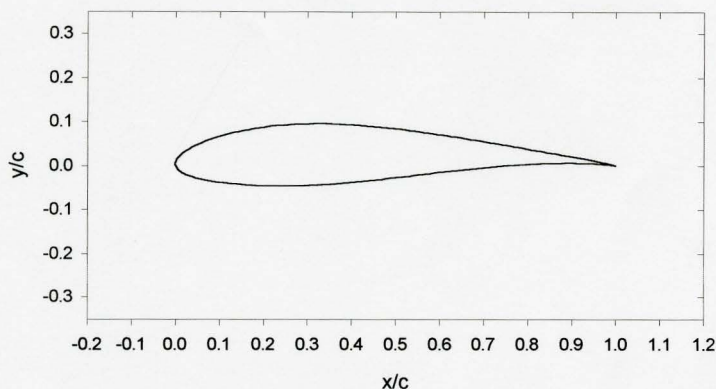


Figure 11--Modified Wartman FX63B Airfoil Shape

Detail Design

Final Performance Data

Takeoff Performance

One of the main constraints of this design problem is the takeoff distance. The airplane must start from rest, takeoff, and clear a six-foot-high barrier within 300 feet. The governing equation is simply Newton's second law including thrust, drag, and rolling friction forces. This second-order differential equation was numerically integrated until the lift equaled the weight, as shown in Figure 12, using a fourth-order Runge-Kutta method as detailed in Appendix B. The thrust using the brush motor, drag, and rolling friction forces are plotted as a function of velocity in Figure 13.

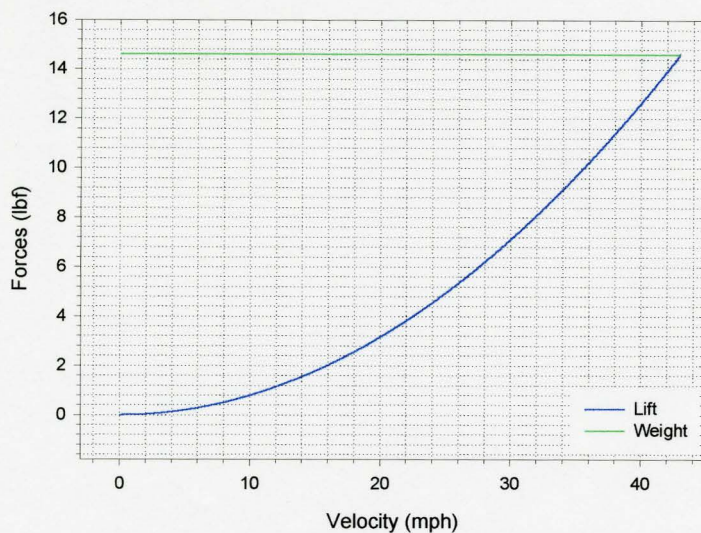


Figure 12--Lift Force and Weight vs. Velocity

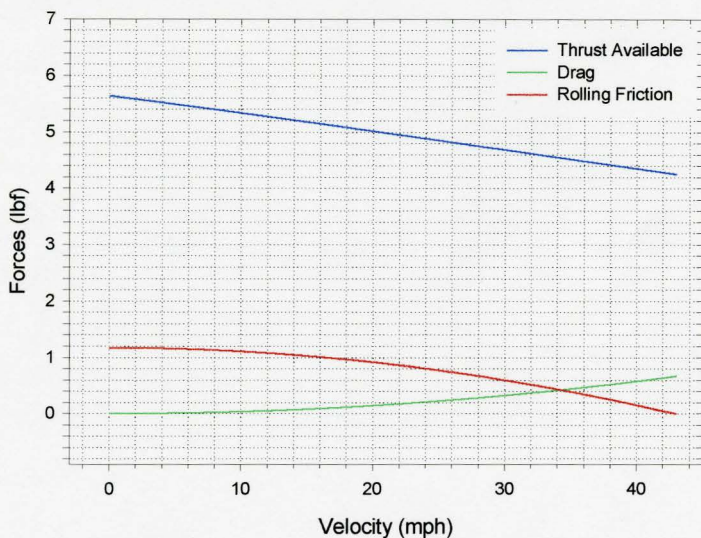


Figure 13--Thrust, Drag, and Rolling Friction Forces vs. Velocity

After finding the distance until the airplane lifts off the ground, the rate of climb was calculated. The remaining distance needed to clear the ribbon was determined using the rate of climb. The values calculated from this analysis are included in the power plant component selection section later. The analysis indicates that the airplane will just takeoff within the 300 feet without the use of flaps, but will easily takeoff with the use of flaps.

Handling Qualities

The airplane's handling qualities are measured by its stability characteristics in pitch, yaw, and roll and by how well the control surfaces are able to maneuver the airplane.

Stability Characteristics

The three restoring moments about the center of gravity cause the airplane to return to equilibrium after it has been disturbed by an outside force. To determine whether or not an airplane is stable in these three

directions, the slope of the moment with respect to angle of attack or sideslip angle must be analyzed. The stability characteristics for this design are summarized in Table 3.

Also, the degree of pitch stability is measured by the stick fixed static margin, which is defined as the distance between the airplane's neutral point and center of gravity divided by the mean chord length of the wing. This value is then converted to a percentage.

$$\frac{X_{NP} - X_{CG}}{\bar{c}} \times 100 = S.M.\% \quad (9)$$

The static margin for any airplane should be at least 10%. For this airplane, it is 25.0%

Table 3--Stability Characteristics

Stability Characteristic	Requirement for slope of moment coefficient	Good Range (deg ⁻¹)	Upper Limit (deg ⁻¹)	Actual Value (deg ⁻¹)
Pitch	$\frac{dC_m}{d\alpha} < 0$	--	--	-0.0263
Roll	$\frac{dC_{ll}}{d\beta} < 0$	-0.001 to -0.002	-0.004	-0.00133
Yaw	$\frac{dC_{ln}}{d\beta} > 0$	0.0015 to 0.0020	--	0.00185

The pitching moment coefficient as a function of angle of attack is shown in Figure 14 and the rolling and yaw moment coefficients as a function of sideslip angle for the design are shown in Figure 14 and Figure 15.

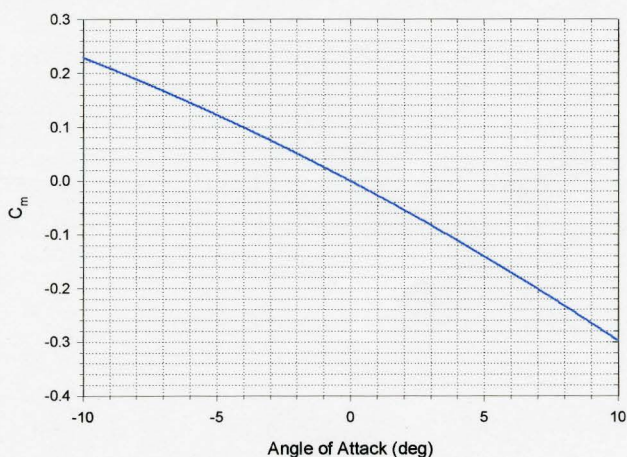


Figure 14--Pitching Moment vs. Angle of Attack

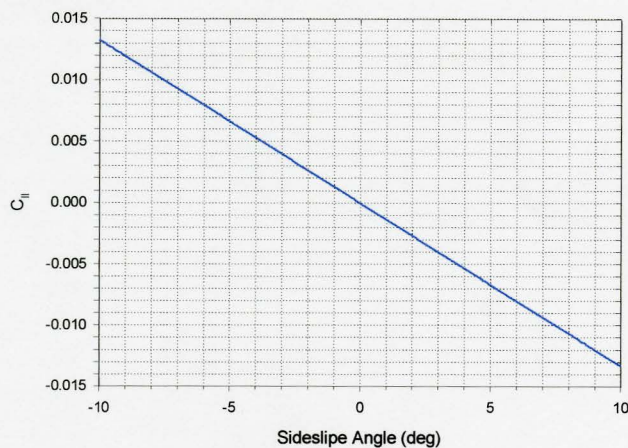


Figure 15--Rolling Moment Coefficient vs. Sideslip Angle

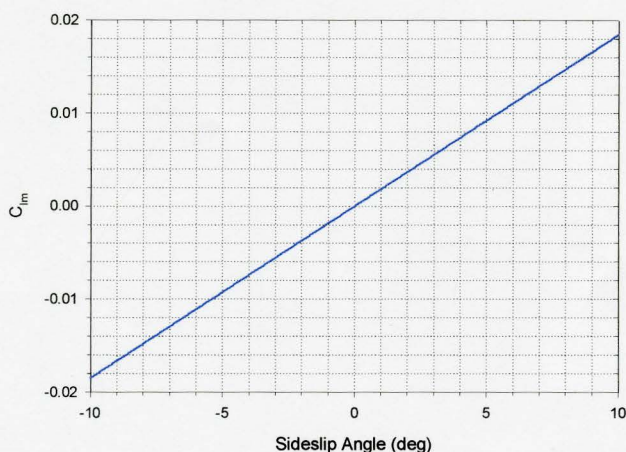


Figure 16--Yawing Moment Coefficient vs. Sideslip Angle

Control Surface Sizing

The ailerons were initially sized using the “rules of thumb” from *Design & Build your own R/C Aircraft*. The book indicates that the ailerons should be 12% of the wing area. Since this airplane design has a large load of steel that increases the moment of inertia, 16% of the total wing area will be ailerons. The “Airplane” program was used to calculate how much deflection would be necessary for ailerons of this size. According to Perkins and Hage, for general aviation aircraft, the dimensionless roll rate should be greater than 0.07 for adequate roll control as shown in Equation (10) (Perkins and Hage):

$$\frac{\omega_{roll} b}{2V_a} \geq 0.07 \quad (10)$$

where ω is the roll rate, b is the wing span, and V_a is the airspeed. For this design, the ailerons must be deflected 17.5 degrees to produce a dimensionless roll rate of 0.07.

The “rules of thumb” indicate that the rudder should be 30% to 50% of the vertical fin area. The book recommends 30% be used if the airplane has a high wing. However, the rudder was sized at 40% to

compensate for the extra control needed to counteract the 7.5 pound payload. The airplane will have a all-flying tail and, therefore, the elevator sizing is not relevant to this design.

Range and Endurance

The range, in terms of number of laps the airplane can complete, is calculated with “Params”. As long as the other necessary design requirements are met, the maximum number of laps is the most important design parameter. The design team used this performance determination as a tool for making decisions throughout the process. Depending on the speed the airplane flies, the range can be limited by the seven-minute time constraint or by available energy in the battery.

This analysis deducts the energy consumed in takeoff, reaching the flying altitude, and completing the first lap with the two 360 degree turns from the total available battery energy. The remaining energy is then used to calculate the number of possible laps as airspeed is varied.

The maximum number of laps for the airplane design using the Aveox brushless motor with a 9x10 propeller is shown in Figure 17. The airplane will run out of time before battery power if flown at airspeeds less than 80 mph and will run out of battery power before time for airspeeds faster than that. The airplane should be able to complete 22 laps if flown between 76 and 81 mph.

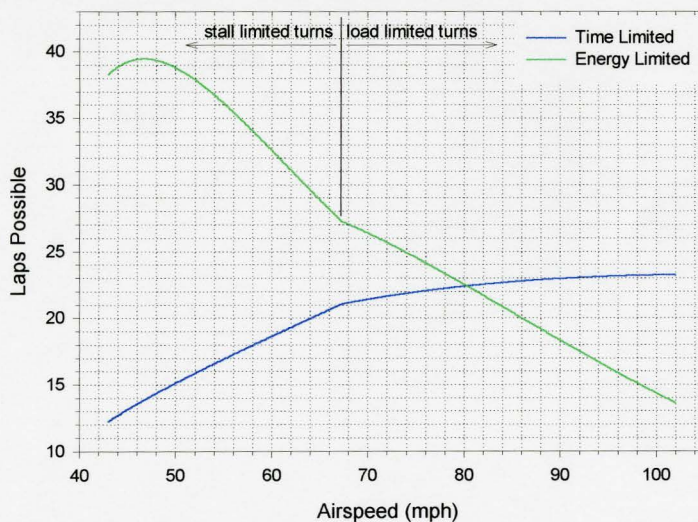


Figure 17--Maximum Number of Laps for Final Design Using Brushless Motor

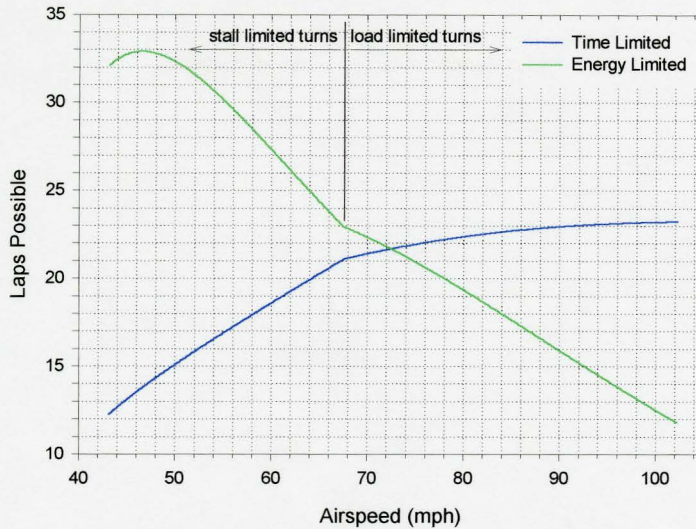


Figure 18--Maximum Number of Laps for Final Design Using Brush Motor

The maximum number of laps for the airplane design using the Astroflight brush motor with a 10x11 propeller is shown in Figure 18. The design is time limited up to about 71 mph and energy limited at speeds higher than that. If the plane flies between 67 and 75 mph, it should be able to complete 21 laps.

G-load Capability

The competition rules state that before flying in the competition the airplane must be able to be lifted by its wing tips without failure simulating a 2.5g load case. Therefore, at minimum, the plane must be able to withstand a 2.5g maneuver. However, as is shown by the plot in Figure 19, by increasing the positive load limit, the airplane can increase the number of laps it can complete in the time limit.

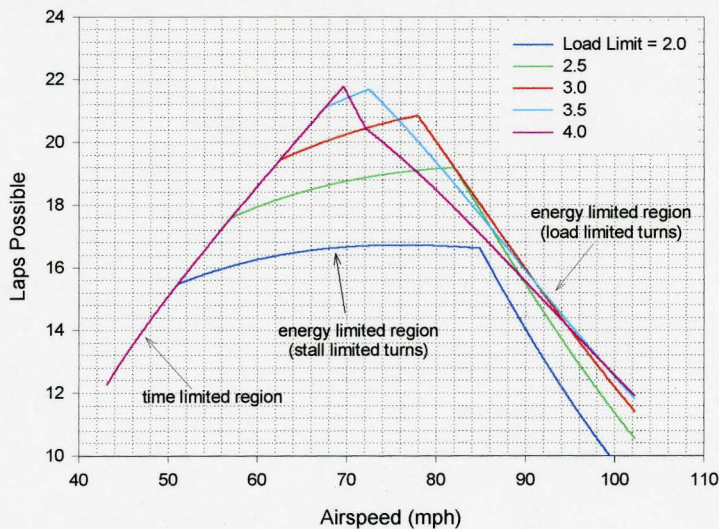


Figure 19--Maximum Number of Laps Varying the Positive Load Limit Using Brush Motor

The calculations for this plot were made assuming the airplane is turning at its minimum possible turning radius. Up to a certain airspeed, the minimum possible turning radius is limited by wing stall and above that airspeed, it is limited by the positive load limit of the airplane. By increasing the strength of the wing, the airplane can spend less time and distance on the turns and therefore increase the number of completed

laps in seven minutes. As is seen by the plot, increasing the positive load limit beyond 3.5g gives little to no benefit. This is because the minimum turning radius is stall-limited before it is strength-limited. Therefore, this airplane was designed to withstand a 3.5g load case.

The tapered box beam in the wing is the primary structural member that must withstand the 3.5g load. To test for this strength, a full scale tapered beam that measures half the span of the wing was constructed. Also, a Styrofoam wing covered with balsa wood and Ultrakote sheeting without an internal beam was constructed to determine the deflections that the sheeting could withstand without buckling. The root end of the wing and the root end of the beam were fixed in a cantilevered arrangement and a load was applied to the free end. An analysis of a simply supported beam indicates that a 3.5g load can be simulated if 87.5% of the total weight of the airplane is applied to each wing tip. Using a conservative weight of 16 lb. it was determined that each wing would have to support 14 lb. In Figure 20, a plot of the tip load versus the deflection indicates that within the safe deflection of the sheeting, the beam itself will have a safety factor of about 2.5. When the strength of the sheeting is added, the safety factor is nearly three.

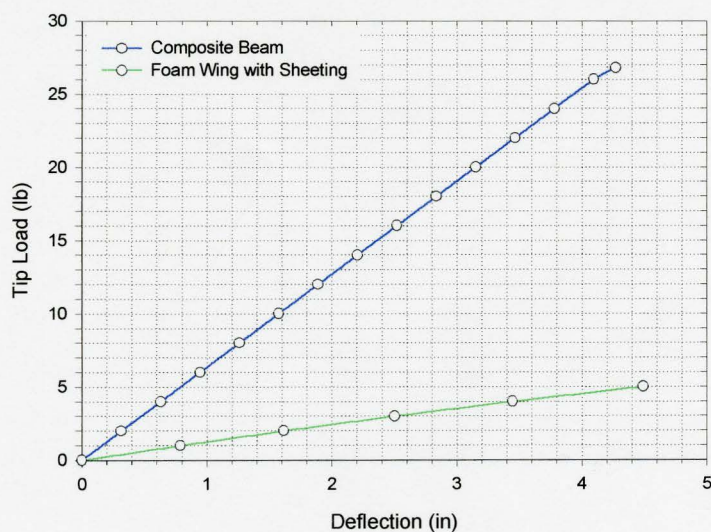


Figure 20--Load-Deflection Curve for Wing

Payload Fraction

At this stage of the design process the weight of the plane is estimated to be 14.57 pounds, which is considerably less than the original requirement of 17 pounds. This makes the weight of the payload to the total weight ratio .515 or 51.5%. The weight of the payload to the dry weight of the airplane 1.061 or 106.1%. Therefore, the payload is over half of the total weight of the aircraft. A more detailed weight analysis is shown in Table 4.

Table 4--Weight Summary

<u>Airframe Structure:</u>	
Fuselage	0.92 lb.
Landing Gear	0.6 lb.
Tail	0.12 lb.
Tail Tube	0.08 lb.
Wings	0.85 lb.
<u>Subtotal:</u>	<u>2.57 lb.</u>
<u>Internal Components and Payload:</u>	
Motor	0.75 lb.
Motor Batteries	2.5 lb.
Motor Speed Control	0.06 lb.
Propeller & Spinner	0.18 lb.
Push Rods	0.06 lb.
Receiver & Servo Package	0.8 lb.
Steel Payload	7.5 lb.
Pitot Tube	0.15 lb.
<u>Subtotal:</u>	<u>12 lb.</u>
<u>Total:</u>	<u>14.57 lb.</u>

Wind Analysis

Figure 21 and Figure 22 show the maximum number of laps that can be completed for different magnitudes of headwind and crosswind. The maximum number of laps are calculated from a strictly time-limited approach, and from an energy-limited approach which takes into account the aircraft drag characteristics, battery capacity, and power-plant energy consumption parameters. From these plots, two major characteristics can be seen:

- 1) The cross wind has larger effect on the optimum airspeed than the headwind
- 2) The optimum airspeed decreases with larger wind speeds

Decreasing the airspeed in a wind may seem counterintuitive. In fact, both the energy limited optimum airspeed and the time limited optimum airspeed increase with wind speed. However, for this design the optimum always occurs at the intersection of the time limited curve and the energy limited curve, and this intersection moves to lower airspeeds with higher wind speeds.

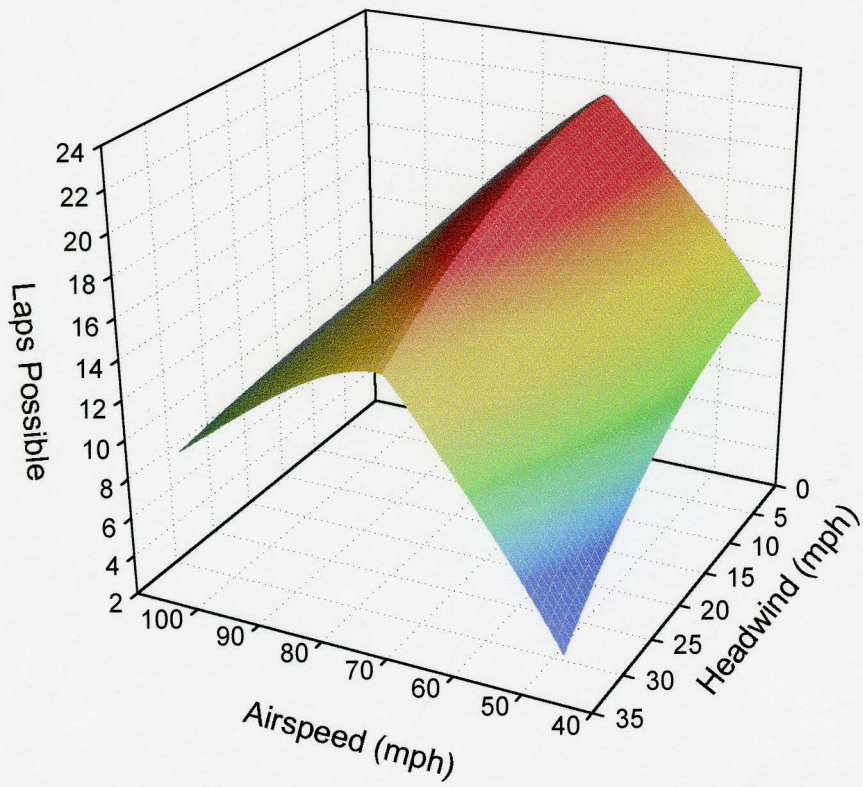


Figure 21--Maximum Number of Laps Varying Headwind Using Brush Motor

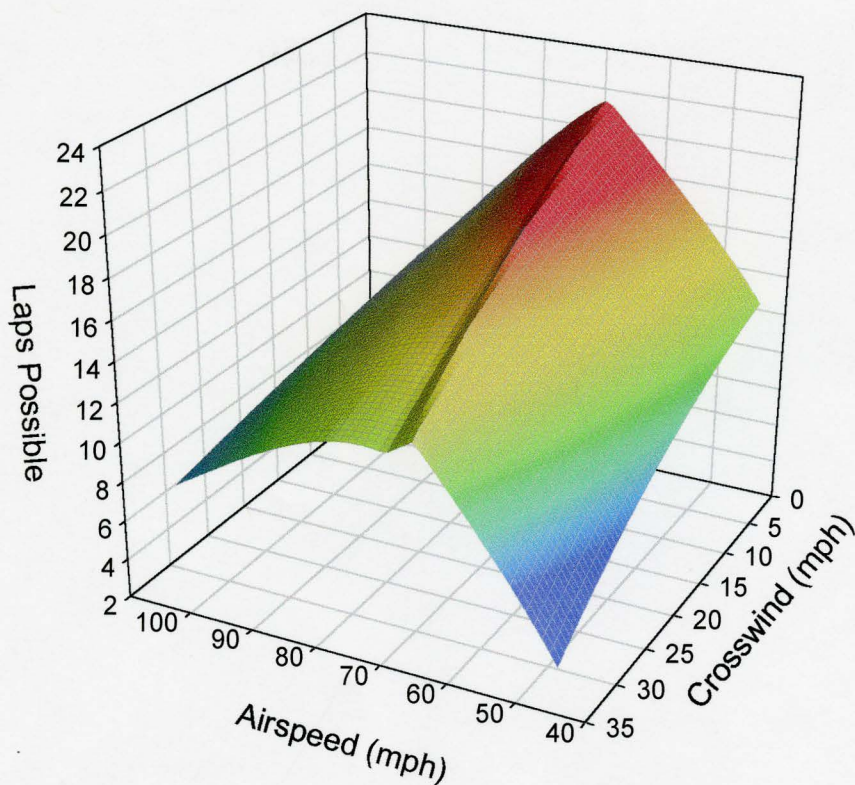


Figure 22--Maximum Number of Laps Varying Crosswind Using Brush Motor

Other Performance Plots

Using "Params," a number of other performance predictions can be made. The lift-to-drag ratio is plotted vs. airspeed for three different altitudes in Figure 23. Note that the maximum for L/D occurs at the minimum drag velocity of 53 mph at Wichita's altitude, as is expected. The maximum L/D requirement of 25 was not achieved because of the necessary sacrifices in wing efficiency made to reduce the planform area to 3.0 ft² as discussed previously.

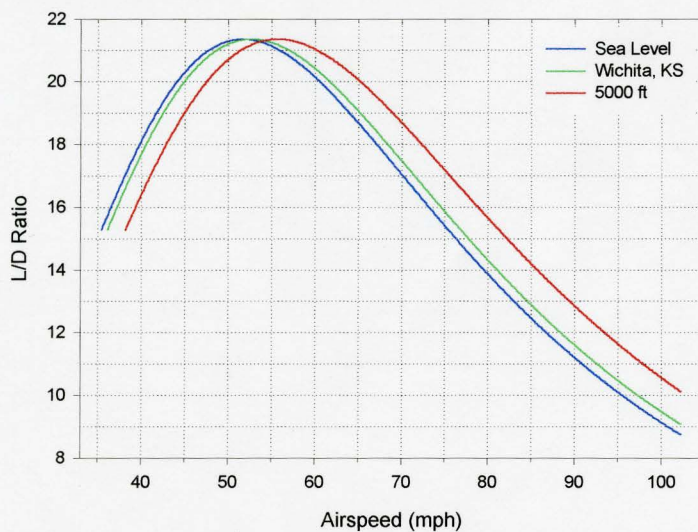


Figure 23--L/D ratio vs. Airspeed

Figure 24 shows the thrust required and the thrust available using the brush motor with 10x11 propeller for throttle settings of 0.4, 0.5, 0.6, and 0.7 as a function of airspeed. The airplane will fly at the airspeed corresponding to the intersection of the thrust required and thrust available curves for a given throttle setting.

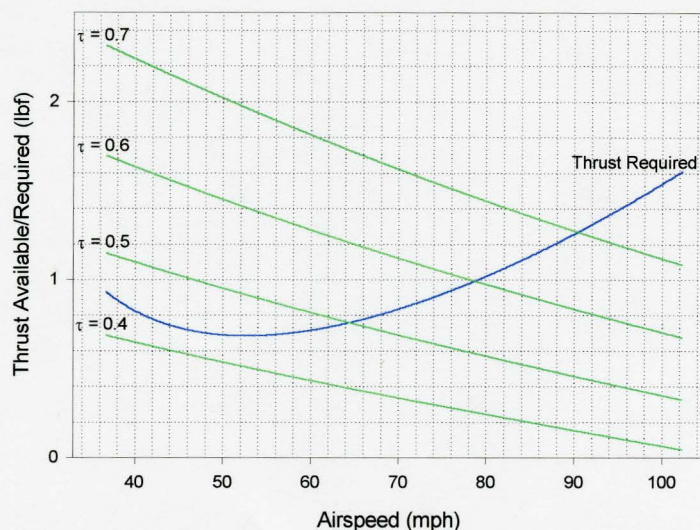


Figure 24--Thrust Available and Thrust Required Using Brush Motor

The throttle setting required for steady, level flight using the brush motor and 10x11 propeller is plotted for varying airspeeds for three different altitudes in Figure 25. Flying at 70 mph will require a throttle setting of about 0.535.

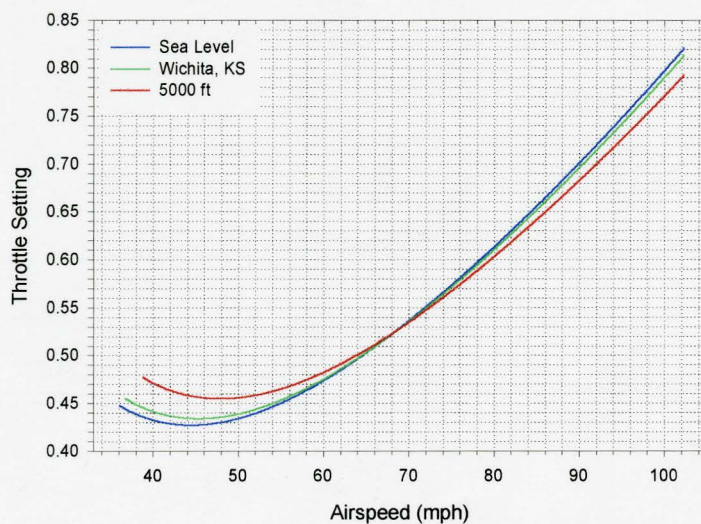


Figure 25--Required Throttle Setting for Steady, Level Flight Using Brush Motor

The minimum turning radius for this design using the brush motor is shown in Figure 26 as a function of airspeed for three different altitudes using a positive load limit of 3.5. For the left-hand section of each curve, the turning radius is limited by wing stall. For the right-hand section of each curve, the turning radius is limited by the strength or positive load limit of the airplane.

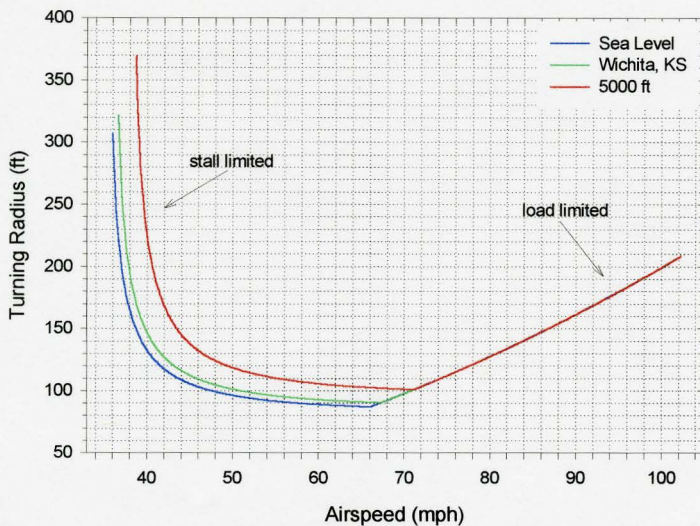


Figure 26--Minimum Turning Radius vs. Airspeed Using Brush Motor

The rate of climb at Wichita's altitude for various throttle settings using the brush motor is shown in Figure 27.

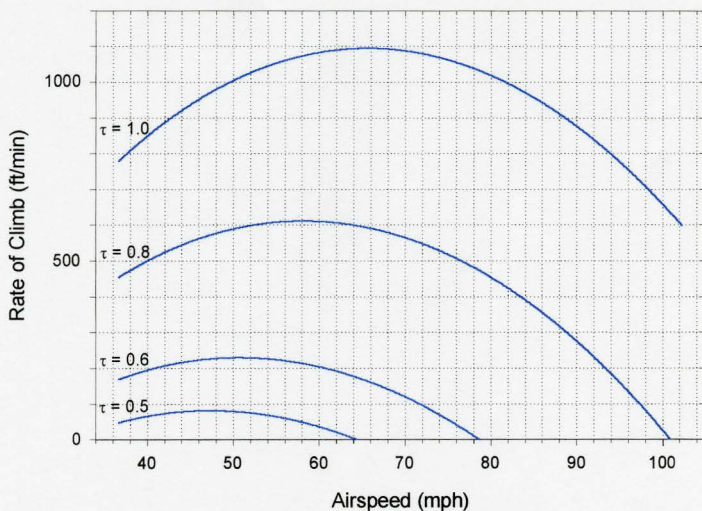


Figure 27--Rate of Climb vs. Airspeed Using Brush Motor

The energy consumption rate in steady, level flight using the brush motor for three different altitudes is shown in Figure 28. The minimum occurs at an airspeed slightly higher than the minimum drag airspeed. This is due to the fact that the power plant efficiency increases with airspeed.

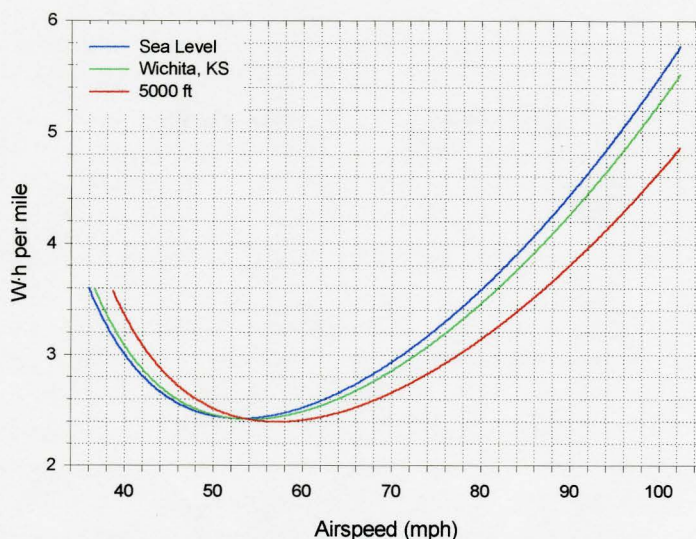


Figure 28--Energy Consumption Rate vs. Airspeed Using Brush Motor

A more useful plot, the energy consumption per lap, is shown in Figure 29. Note that it is not always most efficient to take turns at the minimum turning radius. This is because for sharper turning radii, the wings must generate more lift. This extra lift causes a significant increase in the induced drag. Also, the most efficient airspeed is less than the minimum drag airspeed. This is due to the fact that the turning radius increases with velocity and therefore more energy is required to travel the extra distance necessary for higher airspeeds on the turns.

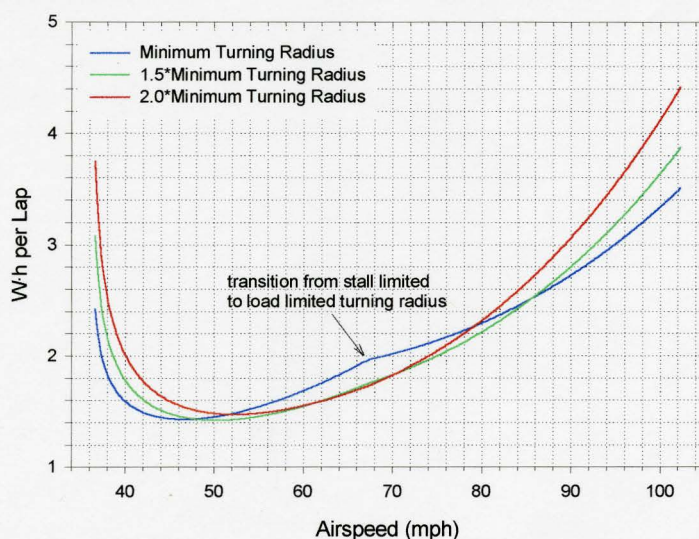


Figure 29--Energy Consumption Per Lap vs. Airspeed Using Brush Motor

Power Plant Component Selection

The “Mpeff” program was used to determine the most efficient motor, propeller, and battery pack combinations for the design. The “Mpeff” program uses information generated by the “Airplane” program about the design’s aerodynamic characteristics and automatically studies the efficiencies of every reasonable motor/propeller combination for a range of airspeeds. The power plant combinations investigated included 24 Aveox brushless motors and 10 Astroflight brush motors using every reasonable propeller from 4 to 16 inches in diameter.

“Mpeff” helped the team determine that a battery pack of about 20 cells is necessary to provide enough power for takeoff. However, exceeding this number of cells by too much requires the motors and speed controls run outside of their safe operating ranges. The battery pack selected includes 19 1.2V Sanyo RC-2300 NiCad cells with a capacity of 2300 mAh per cell. This battery pack will provide 52.44 Watt-hours of energy. The calculations demonstrated that this 22.8 Volt battery pack would provide the needed power for takeoff. Many other battery pack configurations were investigated, but this chosen combination provided the most energy in 2.5 pounds for battery packs with approximately 20 cells.

The “Mpeff” program was used to narrow the selection of power plant combinations. Both a combination using an Aveox brushless motor and speed control and a combination using an Astroflight brush motor was determined that meet the design requirements for this airplane. “Mpeff” performs a rough take-off analysis and eliminates the combinations that do not provide sufficient power for take-off. The overall efficiencies of the remaining motor, speed control, propeller, and battery pack combinations were studied over a range of airspeeds and “Mpeff” determined the motor/propeller combinations that provide the best efficiencies. In addition, the current levels of the remaining possible combinations were examined to make sure the maximum current limitations specified by the manufacturer are not exceeded.

The best combinations, as determined by “Mpeff,” were then run through the more thorough takeoff analysis in “Params” to make sure that they can actually lift off in the required distance. The best Astroflight brush motor for this airplane is the 625G motor with a 1.63:1 gear ratio and a 10x11 propeller, which gives an overall efficiency of 58.1% at 70 mph. This motor/propeller combination can takeoff in 260 feet without flaps and in 210 feet with flaps deflected at 5 degrees. The maximum current for this combination is 40.5 amps which is slightly above the maximum current rating of 35 amps for this motor. However, the current will only exceed this limit briefly during takeoff, so there should not be any problem. The motor current during steady flight at 70 mph is only 16.4 amps. The best speed controller for this motor and battery pack is Astroflight’s model 210. This has a maximum current rating of 45 amps and can handle up to 19 NiCad cells. This motor will also work well with 10x12, 11x11, and 11x12 propellers. The power plant efficiencies for this combination with all four propellers are shown in Figure 30.

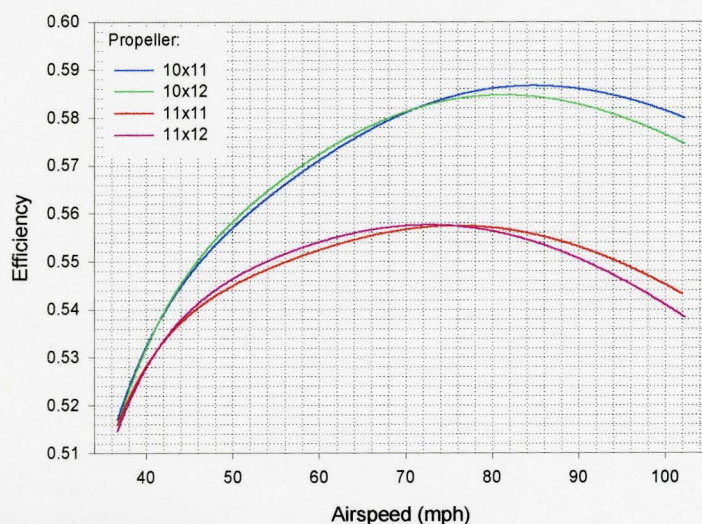


Figure 30--Power Plant Efficiency vs. Airspeed for Four Propellers Using Brush Motor

The best Aveox brushless motor for this airplane is the ungeared 1412/4Y with a 9x10 propeller which gives an overall efficiency of 67.4% at 70 mph. This system will lift the airplane off and clear the six-foot barrier in 250 feet without using flaps and in 203 feet with flaps deflected at 5 degrees. The maximum current draw for this combination is 41.5 amps which is less than the maximum current rating of 50 amps for this motor. While flying in steady flight at 70 mph, this combination will draw 14.8 amps which is less than the continuous current rating of 22 amps. The best speed controller for this setup is the H60 model from Aveox. This controller can easily handle 19 NiCad cells and has a maximum current rating of 60 amps. Other good propellers to use for this system include 9x9, 10x10, and 10x11.

As is discussed in the Conceptual Design section, the brushless motor system costs more than the brush motor system. The performance of both systems was evaluated and as shown in Figure 17 and Figure 18, the airplane can complete 22 laps with the brushless combination and 21 laps with the brush motor combination. The design team did not feel that one extra lap could justify the extra cost, so the brush motor system was chosen at this stage.

Drawing Package

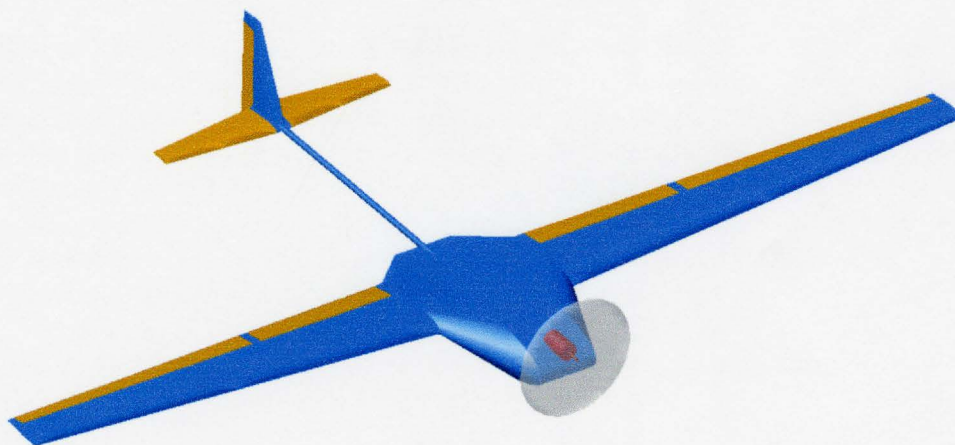


Figure 31--The Airplane

The airplane design was modeled using the SDRC Ideas software package. Figure 31 shows a picture of the completed airplane design. Detailed drawings of the airplane's overall dimensions and fuselage component layout are contained in Appendix C.

Manufacturing Plan

Wing Construction

Beam

The manufacturing process for the carbon fiber composite box beam in the wing began with the laying up of the fiber composite laminates. Unidirectional pre-preg carbon fiber material was selected for the construction of the beam. The pre-preg material and the facilities to lay up the carbon fiber sheet are readily available at Utah State University, which made possible the construction and use of the fiber composite material. A large sheet of the carbon fiber composite material was laid up and the carbon fiber runners for the beam were cut to exact dimensions. The laminae were laid up as shown in Figure 32, with orientations calculated to oppose the stresses that the beam will experience. The majority of the plies are

oriented in the longitudinal direction to compensate for the large bending moment on the wing. The composite sheet was laid up with an effort to maintain cleanliness and was then vacuum packed to remove voids in the material. Both of these efforts helped to increase the strength of the fiber composite material. After the composite was laid up, it was cured in a large oven.

0°
0°
90°
0°
45°
-45°
0°
90°
0°
0°

Figure 32 – Orientation of Pre-preg Composite Laminae

Using a circular saw and a blade designed to cut ceramic materials, the composite sheet was cut into one-half inch wide strips. These strips were then cut to the proper lengths for the construction of the beam for the wing. The best adhesive found to attach the composite material to the aircraft plywood webbing was epoxy. Jet Instant glue, which is popular among modelers, was also tried but it did not perform well with the composite runners and was hard to work with. The difficulties encountered with the construction of the first prototype box beam demonstrated the value of using a jig. The box beam was not completely square and when the beam was tested, there was significant twist. A wood jig was designed, constructed, and placed inside the beam while it was being assembled to ensure good tolerances. The jig was wrapped in wax paper to allow the jig to be removed after the adhesive finished curing. The epoxy used with the composite beam needed an extended amount of time to cure. To hold the components of the beam in place while the epoxy cured, elastic bands were wrapped around the beam.

At the center of the beam, a balsa wood member was constructed to fill the hollow box portion of the beam located in the fuselage. This provided a solid section to attach the fuselage beam to the wing beam.

Foam Core

Surrounding the beam in the wing is a foam core that gives the wing its airfoil shape. An alternative construction technique was investigated that used balsa wood airfoil shaped ribs covered by Ultrakote. The balsa rib concept was eliminated because of the irregular surface that the ribs create in the Ultrakote. The irregular surface would degrade the aerodynamic performance of the wing.

A low density polystyrene was selected to minimize weight. The foam for the wings was cut using a hot wire cutter according to the following sequence. First, an outline of the planform area of the wing was cut from the Styrofoam. Then, a one-half inch portion was cut out of the Styrofoam to allow room for the main support beam. Next, the flaps and ailerons were cut out and left in the main foam block. Finally, the airfoil shape was cut out using airfoil templates attached to the Styrofoam. This procedure allowed for clean and accurate cuts on all portions of the wing. The scrap Styrofoam pieces that surrounded the cutout airfoil shape were saved for future use.

The airfoil templates for the Styrofoam were originally cut from scrap pieces of balsa and plywood. This proved to be insufficient for a couple reasons. First the wood templates were difficult to construct to high

tolerances. This was a particular problem as the size of the airfoils decreased, particularly at the wing tips. Also, the wood was not an ideal surface to run the wire cutter along because the wire hangs up on the wood causing a poor surface finish on the Styrofoam. To counter these problems, aluminum airfoil templates were machined using a CNC mill which achieved excellent tolerances and gave a smooth surface for the wire to run across.

After the Styrofoam was cut to the proper shape, it was attached to the beam and made ready for application of balsa sheeting and Ultrakote.

Balsa/Ultrakote Sheeting

The sheeting on the wing is primarily to create a smooth surface that allows the airflow to remain laminar as long as possible. Secondary purposes of the sheeting include protecting the Styrofoam and adding strength to the wing.

The sheeting used was 1/32-inch thick balsa. The sheeting was wrapped around the wing with the grain of the balsa lined up with the longitudinal direction of the leading edge of the wing. 3M Spray Adhesive was used to attach the balsa to the Styrofoam and beam assembly. To hold the balsa securely in place while the adhesive set up, the scrap pieces of Styrofoam saved from the airfoil cutting process were fastened around the balsa wood and wing assembly. Ultrakote was applied to the balsa wood sheeting using a custom sealing iron to create a smooth, aerodynamic surface.

Control Surfaces

The control surfaces were made of a foam core with balsa sheeting and Ultrakote covering similar to the wing. The foam core was the section of foam cut out from the wing as mentioned previously. It was sheeted with 1/32 inch balsa, and covered with Ultrakote. The control surfaces were then placed back into position and were hinged to the wing. The control surfaces were attached to the wing with small nylon hinges and a layer of Ultrakote. The hinges maintained the control surface's alignment with the wing while the Ultrakote sealed both the top and bottom of the joint so that air flow between the control surface and wing was not possible. This method of hinging the control surfaces maintained the favorable pressure gradient between the top and bottom of the wing. The servos for the ailerons were placed in each wing and push rods extended to the aileron to control it. The servo for the flaps was placed inside the fuselage and the push rods were directed to the flaps through the wing.

Fuselage Construction

Frame

Due to the ease of construction and the cost of materials, the fuselage was constructed similarly to the wing. The fuselage was uniquely shaped and constructed to increase the aerodynamic performance. The shape of the fuselage is a symmetric airfoil which transitions smoothly on both sides to the cambered airfoil used for the wing. Following the same hot wire method outlined in the wing section, the fuselage was cut out of foam and glued with 3M Spray Adhesive to the wing beam. The electronic components and payload are carried in a section defined by two airfoil-shaped bulkheads. The bulkheads are five inches apart inside the fuselage as shown in the drawing 6 in Appendix C. These bulkheads were cut from 3/32-inch aircraft plywood and are the main support structure for all of the fuselage components. Wooden dowel stretchers extend between the two bulkheads providing a shelf-like structure to which the majority of the components are attached. Most of the components are attached by conventional means. However, the motor batteries are attached with Velcro to allow the batteries to be moved easily to adjust the center of gravity location.

Access Hatch

The fuselage has a hatch that opens from the top to provide access to the payload and electronic components of the plane. The hatch was cut out of the foam and coated with balsa and Ultrakote. A strip of Ultrakote was used to attach the access hatch to the fuselage. This piece of Ultrakote acts as a hinge. When the hatch is closed it is secured by using electrical tape to tape down the free edges of the hatch.

Motor Mount

The motor mount is attached to the bulkheads in the fuselage. The motor is connected to the bulkheads by hardwood dowels. There are two spars that run up next to the motor and the motor is connected to the spars using two nylon wire ties. The hardwood dowels were tested to determine their material properties. Using these material properties, an analysis on the motor mount was done which indicated that the stresses are well within safe limits. Perhaps more importantly, according to the analysis the deflection that the motor mount experiences as a result of the thrust force will be extremely small. This ensures that the direction of thrust remains constant in relation to the orientation of the airplane. Overall, the motor mount is lightweight, simple to construct, inexpensive, and allows motors of various dimensions to be used.

Beam to Tail

To connect the tail to the fuselage, there is a 0.352-inch composite tube that runs from the beam in the wing to the tail of the plane. The tube mounts directly to the beam running through the wings using an aluminum bracket centered in the fuselage. The tube runs back to the tail, which is 26 inches from the beam. The vertical and horizontal surfaces of the tail are attached to the tube with epoxy. The composite tube was the ideal selection because it is light, strong, and initially allowed the push rods from the servos in the fuselage to run inside of the tube to the tail control surfaces. Additionally, the composite tubes are readily available for only seven dollars from a kite hobby shop.

Landing Gear

The main landing gear selected was Hallco-brand Temper-Lock Landing Gear model HALQ2130. The maximum airplane weight for this landing gear as specified by the manufacturer is 10.0 pounds. This design exceeds that by nearly five pounds, so the landing gear was modeled using SDRC Ideas and a finite element analysis was performed. The analysis showed that the stresses incurred during a moderate landing are well below the yield strength of the heat-treated aluminum alloy landing gear. The weight limitations specified by the manufacturer obviously include a safety factor and are designed to withstand a lifetime of hard landings. The landing gear for this application only needs to withstand a few weeks of testing and the competition. A small tail-dragger wheel was attached to the rudder of the airplane. The small wheel was selected over a wire since the wheel will allow easier maneuverability on the ground.

Tail Construction

Based on the information and experience gained during the analysis and construction of the wing, both the horizontal and vertical tail surfaces were constructed with a foam core covered with 1/32 inch balsa sheeting and Ultrakote. Because the loads on these surfaces are not as high as those placed on the wing, these surfaces do not have a main support beam.

The horizontal surface is all flying, with a pivot point located at its quarter-chord. This type of surface was chosen primarily for its ease of construction, reduction in weight, and low material cost. A push rod runs from a servo in the fuselage to a lever arm, which provides the torque needed to move the surface.

The vertical surface was attached to the fuselage-to-tail tube with epoxy. A 90° triangle was used to ensure the proper alignment between the horizontal and vertical surface. The control surface was constructed in the same manner as the wing control surfaces. The servo for the rudder is inside the fuselage and a push

rod runs from the fuselage, through the composite tube, to the rudder. Ultrakote acts as a hinge and attaches the rudder to the vertical stabilizer.

Cost of Designed Airplane

Considerable consideration was given to reducing the cost of the airplane throughout the design process. As much as possible, the design team tried to develop a low-cost design in terms of materials used and manufacturing processes. A detailed breakdown of the costs of the individual components in the final design is shown in Table 5. All costs are based on manufacturer's suggested retail prices (MSRP).

Table 5--Manufacturing Cost Analysis

<u>Airframe Structure:</u>	<u>MSRP</u>
Aircraft Plywood 1/32"	16.00
Aircraft Plywood 3/32"	10.95
Balsa Wood Sheeting 1/32"	37.50
Balsa Wood Supports	3.50
Carbon Fiber Prepreg	25.95
Carbon Fiber Tail Tube	7.00
Hard Wood Dowels 3/16" & 1/4"	0.75
Hinges	1.50
Landing Gear Mount	1.00
Monokote	36.00
Motor Support Clamps	0.80
Plastic Bolts & Nuts 3/8"	4.00
Scotch Tape	1.29
Styrofoam	15.75
Tail Gear	3.00
Tail Tube Support Bracket	1.89
Tail Tube Support Clamps	0.80
Wheels & Collars	7.00
	<u>Subtotal:</u> 174.68
<u>Internal Components and Payload:</u>	
Motor	125.00
Motor Batteries	115.15
Propeller & Spinner	30.00
Push Rods	8.25
Radio & Receiver Package	350.00
Speed Controller	65.00
Steel Payload	3.83
	<u>Subtotal:</u> 697.23
<u>Construction Supplies:</u>	
Aluminum Templates	1.95
Balsa Filler	10.89
Epoxy	15.95
Glue Accelerant	5.29
Masking Tape	0.79
Rubber Bands	1.98
Spray Glue	12.33
Wood Glue	20.98
Wood Jigs	5.00
	<u>Subtotal:</u> 75.16
	<u>Total:</u>
	<u>\$947.07</u>

Manufacturing Milestone Chart

The scheduled event timings are detailed below in Figure 33.

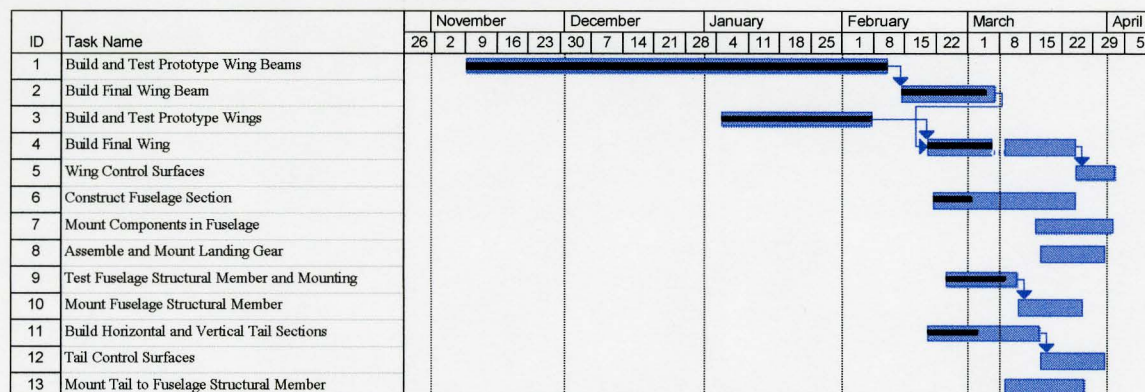


Figure 33--Manufacturing Milestone Chart

Flight Testing

Push Rods

Once construction of the airplane was completed, a number of test flights without the payload were performed to see how the airplane handled. For the most part, the airplane performed well, but it was discovered that there were problems with hysteresis in the all-flying tail movement. This made it extremely difficult for the pilot to trim the airplane for steady flight. The design team determined that the hysteresis was caused by compression of the braided cable used in the push rods. This problem was remedied by replacing the braided cable push rod with a 1/16 inch diameter steel push rod which ran inside a plastic tube.

Landing Gear

Another problem discovered during the test flights was that the landing gear selected was not strong enough. Once on takeoff and once on landing, the landing gear described in the Manufacturing Plan section bent out of shape beyond repair. As a result, a larger, and stronger landing gear was chosen. This increased the drag slightly, but it was a necessary change.

Power Plant

Once the airplane was performing well without the payload, an attempt was made to takeoff in 300 feet with the payload. As indicated earlier, the analysis showed that the airplane should be able to take off in 260 feet without flaps. The airplane was nowhere near accomplishing that. This led the team to believe that there were some problems with the power plant analysis.

In general, the design team feels that the mathematical model used to describe the motor, speed controller, and battery pack, as shown in Figure 5 (also see Appendix A), has been well tested and closely predicts the combined performance of these elements of the power plant. However, since the mathematical equations used to describe the performance of the propeller in this program were derived from very limited information gathered from one source, the design team suspected that the performance results of the propellers predicted by "Mpeff" were not correct.

The design team compared the predicted propeller characteristics calculated by “Mpeff” with experimental data. Jim Fufarro, a graduate student at Utah State University, tested several propellers in a low speed wind tunnel with the use of a single motor and a direct voltage source. Two plots comparing the experimental data collected during this test with the results of “Mpeff” are shown in Figure 34 and Figure 35. From these two plots, it can be seen that the “Mpeff” program predicts a higher thrust output than the actual thrust output measured experimentally. The difference between the thrust output results was significant enough to warrant a change in the power plant design. Further study of the experimental data will help the design team correct the mathematical equations that describe the propeller performance and update the “Mpeff” program so that it more closely approximates the experimental data.

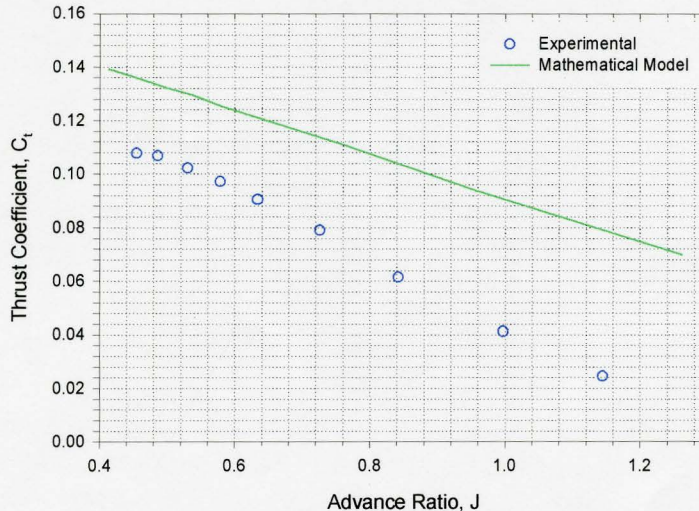


Figure 34 -- Thrust Coefficient vs. Advance Ratio for 11x11 Propeller at an Airspeed of 35.5 MPH

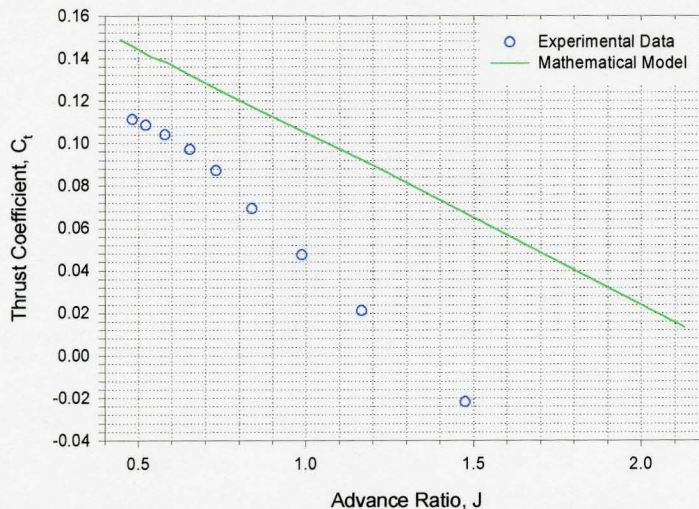


Figure 35 -- Thrust Coefficient vs. Advance Ratio for 11x12 Propeller at an Airspeed of 35.5 MPH

In addition, the static thrust of the Astroflight 625G brush motor with a 12x12 was measured at full throttle and did not exceed two pounds. According to the propeller data used in “Mpeff”, this propeller/motor combination should provide over 6 pounds of static thrust at full throttle. The design team determined that

this motor could not provide enough thrust to takeoff with the payload. As a result, an ungeared Aveox 1412/4Y brushless motor and speed controller were purchased.

Wing Size

Once it was discovered that the brush motor system would not provide enough thrust to takeoff, only one week remained before the competition. If there had been more time, more flight tests would have been performed with the brushless motor system before making drastic changes to the airplane design. However, there was not time for more extensive flight testing, so the design team decided to rebuild the wing with a planform area of 4.0 ft². This was accomplished by maintaining a root chord length of eight inches and increasing the tip chord length from four to eight inches. These changes reduced the efficiency of the wing, but provided a significant increase in the lift of the wing. The computer analysis was performed on this new design and it was verified that it was still balanced properly.

With the new brushless motor and larger wing planform area, a couple more flight tests were performed. The airplane was able to take off with the payload in the 300 feet and handled very well in flight. However, the design team still feels that given enough time, the airplane design with a 3.0 ft² wing area could work as well. Once made to work, the airplane with the smaller wing area is a better design.

Competition

Design Report

As discussed earlier, the design report was scored out of 100 points. Utah State University was awarded the highest score on this portion of the competition with 91.9. That put Utah State in first place going into the actual flying portion of the competition.

Fly-Off

The flying conditions in Wichita on the day of the competition were terrible. The runway was oriented in the north-south direction and was only about 15 feet wide. For most of the day, gusting winds ranging from 15 to 30 mph came out of the south. As the day went on, the wind slowly shifted to a cross-wind coming out of the west.

These conditions proved to be disastrous for most of the teams in the competition. Only four teams out of 17 were able to make any qualifying laps and land on the runway without crashing. Utah State's airplane crashed on landing on the first attempt. The rest of the day was spent repairing the airplane. Just before the runway was closed for the competition, one last attempt was made, but the airplane was blown off the side of the runway due to the severe crosswinds.

Areas for Improvement in Next Design

Tail Boom Design

During initial flight tests, a few problems with interference between the radio and receiver while the motor is running were discovered. It was found that the interference was worse when the antenna was placed near the carbon fiber in the main support beam of the wing and the carbon fiber tail boom. Therefore, a possible remedy to this problem is to use a different material for the tail boom so the antenna can be run through it.

The small carbon fiber tube used for the tail boom was extremely successful in decreasing the weight of the airplane. However, it became evident during test flights that it was not stiff enough in bending or in torsion. The lack of resistance to torsion allows the tail section to twist about the main axis when rudder is

applied in flight, but does not significantly affect the airplane's performance. The lack of stiffness in bending causes the boom to deform when elevator was applied in flight. This causes serious control problems at high airspeeds, and had to be corrected by reinforcing the tail boom at the trailing edge of the fuselage. A future design would be improved by increasing the stiffness of the tail boom in both bending and torsion, even at the cost of added weight.

Main Support Beam in Wing

As is documented in the proposal phase of the Design Report, the main support beam in the wing was designed to withstand a 3.5g load. The beam was tested for strength and it was discovered that the beam can withstand that loading with a safety factor of three. Therefore, the main beam could be made smaller and lighter in a future version of the wing. The size of the beam in the current design caused some difficulties in maintaining the proper airfoil shape in the wing sections. Thus, reducing the beam size would also provide benefits in the aerodynamic performance.

Easy Modifications

One definite improvement for a future design is to allow for easier access, modification, and repair of the various components of the airplane. Some items are permanently built into the structure, so in order to access them, parts of the airplane would have to be disassembled.

Battery Pack

When the 19-cell battery pack was ordered from the manufacturer, it was clearly stated by the design team that the finished weight was to be less than 2.5 pounds. Upon inspection of the delivered product, it was found that the manufacturer had cut a few corners in order to meet this weight requirement. Most noticeably, the connectors between the individual cells are too small, causing excess internal losses and generating much heat. To prevent this from occurring in a future iteration, the design team would find a battery pack manufacturer here at Utah State University so that closer control could be maintained over the manufacturing process.

Control Surfaces

When the wing was rebuilt with 4.0 ft², the flaps and ailerons were constructed out of solid balsa wood rather than using a foam core. The solid balsa was not only easier to work with but also produced surfaces with much tighter tolerances. In the future, better control surfaces could be built in less time using the solid balsa approach.

References

- Abbott, Ira H. and Von Doenhoff, Albert E., *Theory of Wing Sections Including a Summary of Airfoil Data*, Dover Publications, Inc., New York, 1959.
- Anderson, John D. Jr., *Fundamentals of Aerodynamics*, 2nd Ed., McGraw-Hill, Inc., New York, 1991.
- Boucher, Robert J., *Electric Motor Handbook*, Astroflight, Inc.
- Perkins and Hage, *Airplane Performance Stability and Control*, Wiley, 1949.
- Smith, Kenneth L. *Design & Build your own R/C Aircraft*, Robson House Hobby Supplies, Edmonton, Alberta, Canada, 1984.

Appendix A--Equations Relating to Power Plant

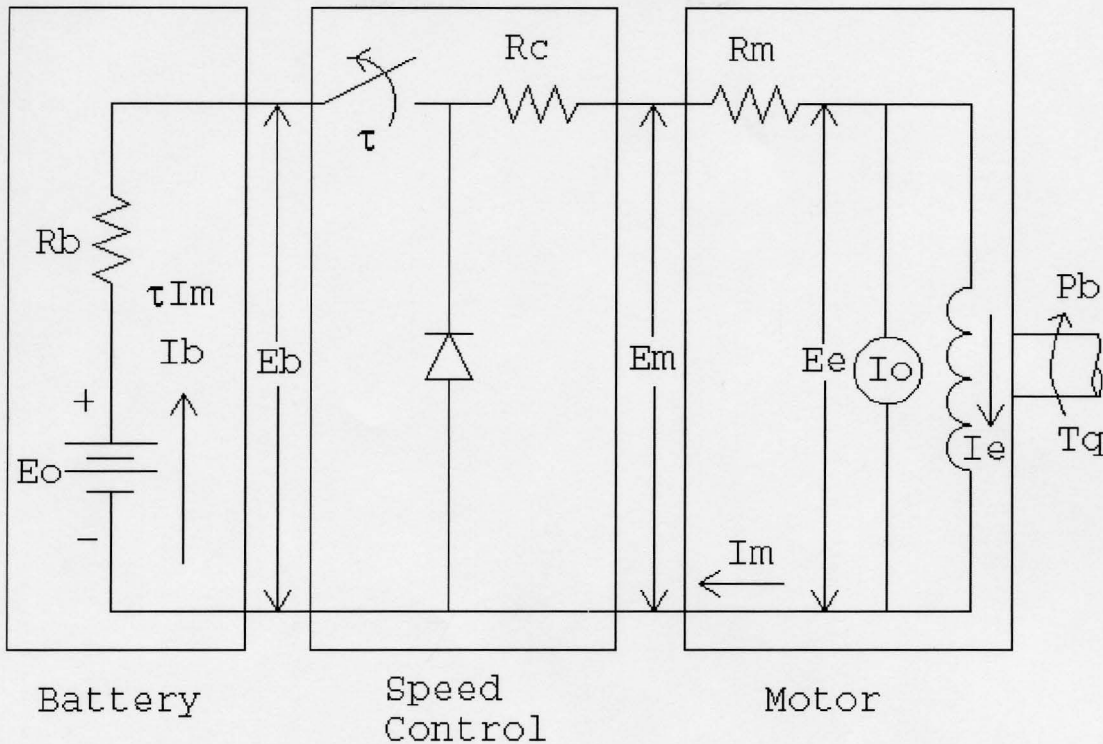


Figure 36--Schematic of Motor/Speed Control/Battery System

The following mathematical relationships for the motor, speed control, and battery are utilized in the "Mpeff" program. Voltage and Current values in equations are labeled on schematic above.

Motor:

Shaft rotational speed (rpm):

$$n = \frac{K_v}{G_r} (E_m - I_m R_m)$$

Output torque of motor shaft (ft-lbf):

$$T_q = \frac{7.0432 G_r}{K_v} (I_m - I_o)$$

where:

K_v = motor voltage constant
(rpm/volt)

G_r = gear ratio of the motor

R_m = internal resistance of the motor

Speed Control:

$$I_b = \tau I_m$$

$$E_m = \eta_s \tau E_b - I_m R_c$$

Speed control efficiency:

$$\eta_s = 1 - 0.078(1 - \tau)$$

where:

τ = throttle setting (0 to 1)

Battery Pack:

$$E_b = E_o - R_b I_m$$

where:

R_b = internal resistance of the battery pack

The power required to turn the propeller shaft and the thrust delivered by the propeller were calculated according to the equations that follow. These equations relate the propeller performance to its pitch and diameter. They were developed from limited empirical data gathered from *Electric Motor Handbook* written by Robert J. Boucher of Astroflight, Inc.

Propeller:

Thrust available:

$$T_A = C_T \rho n^2 d^4$$

Break power required:

$$P_b = C_p \rho n^3 d^5$$

Torque required:

$$T_q = \frac{C_p}{2\pi} \rho n^2 d^5$$

Propeller efficiency:

$$\eta_p = \frac{T_A V_a}{P_b}$$

Advance ratio:

$$J = \frac{V_a}{nd}$$

Thrust Coefficient:

$$C_T = C_{T_o} - C_{TJ} J$$

Power Coefficient:

$$C_p = C_{p_o} + C_{pi}$$

$$C_{T_o} = \begin{cases} 0.4077 \frac{P}{d} - 0.36625 \left(\frac{P}{d} \right)^2; \frac{P}{d} \leq 0.40 \\ 0.0586 + 0.1147 \frac{P}{d}; \frac{P}{d} \geq 0.40 \end{cases}$$

$$C_{TJ} = \begin{cases} 0.524185 - 1.72181 \frac{P}{d} + 1.78940 \left(\frac{P}{d} \right)^2; \frac{P}{d} \leq 0.46 \\ 0.142503 - 0.0760669 \frac{P}{d} + 0.0154988 \left(\frac{P}{d} \right)^2; \frac{P}{d} \geq 0.46 \end{cases}$$

$$C_{p_o} = 0.00868 + 0.00450 \left(\frac{P}{d} \right)^2 + 0.01643 \left(\frac{P}{d} - J \right)^2$$

$$C_{pi} = \frac{1}{2} C_T \left(J + \sqrt{J^2 + \frac{8}{\pi} C_T} \right)$$

where:

 ρ = air density p = propeller pitch d = propeller diameter V_a = airspeed

Appendix B—Takeoff Analysis

The governing equation for the takeoff analysis is simply Newton's second law. This equation is represented by the following pair of first order differential equations for the velocity, V_a , and distance traveled, x :

$$\frac{dV_a}{dt} = \frac{g}{W} (T_a - D - F_r) \quad \frac{dx}{dt} = V_a$$

where g is the gravitational constant, W is the weight, T_a is the thrust available, D is the drag, and F_r is the rolling friction force.

The thrust available, T_a , as a function of velocity for this airplane using the Astroflight 625G motor with a 10x11 propeller is shown in Figure 37 below. A polynomial expression for T_a was generated from a least squares fit of this plot.

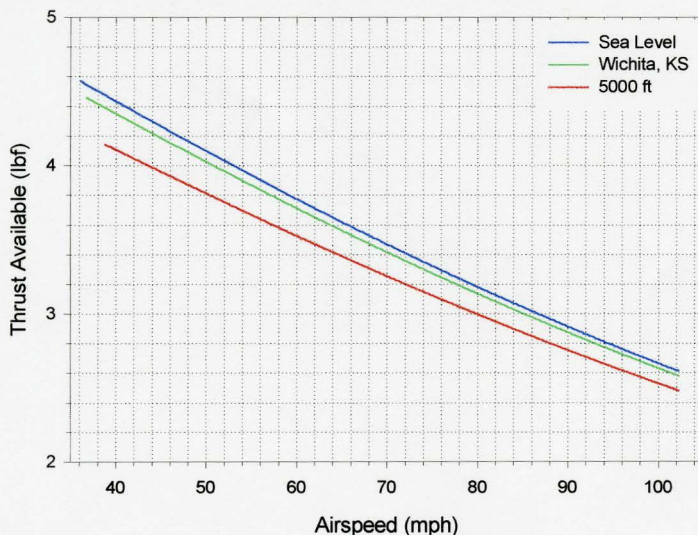


Figure 37--Thrust Available vs. Airspeed

The induced drag on the airplane during takeoff is reduced because the trailing vortices interact with the ground. An empirical correlation factor is included and the relationship for drag is:

$$D = \frac{1}{2} \rho V_a^2 S \left(C_{D0} + \frac{(16h/b)^2}{1 + (16h/b)^2} \left(C_{DL0} C_L + \frac{C_L^2}{\pi e AR} \right) \right)$$

where h is the height of the wing above the ground and b is the wingspan.

The rolling friction force is calculated according to:

$$F_r = \mu_r (W - L) = \mu_r \left(W - \frac{1}{2} \rho V_a^2 S C_L \right)$$

where μ_r is the coefficient of rolling friction. The design team performed experiments on a surface similar to a typical runway with a typical landing gear apparatus and determined that this coefficient is approximately 0.08.

The lift coefficient was assumed to be reasonably constant and it was assigned a value of 70% of the maximum lift coefficient at stall. The chosen airfoil has a maximum lift coefficient of 1.53 with no flap deflection and 1.90 with only 5 degrees flap deflection. The liftoff velocity, V_{LO} , is the airspeed that the lift just equals the weight for this value of the lift coefficient.

$$V_{LO} = \frac{\sqrt{2}}{\sqrt{0.7C_{L_{max}}}} \sqrt{\frac{W}{S \rho}}$$

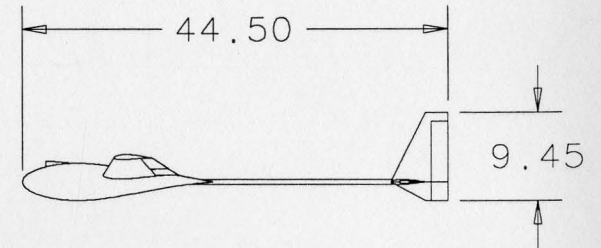
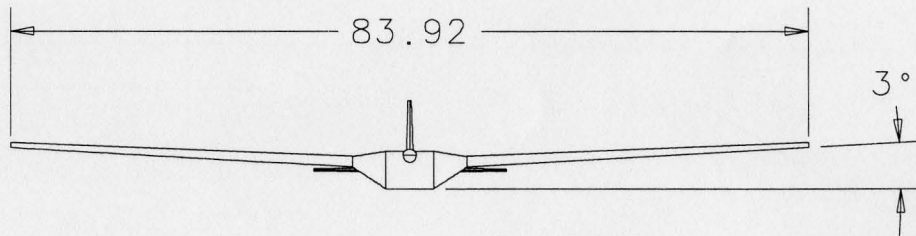
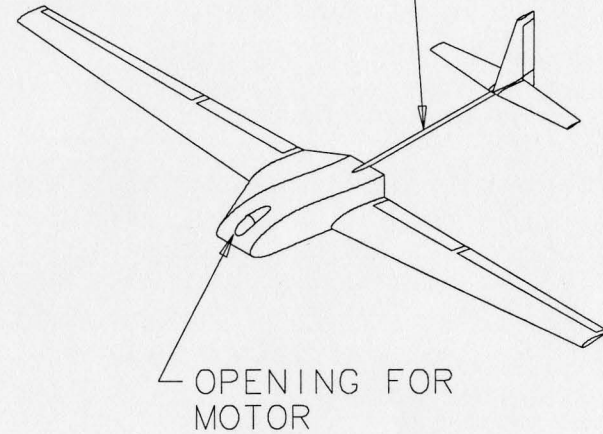
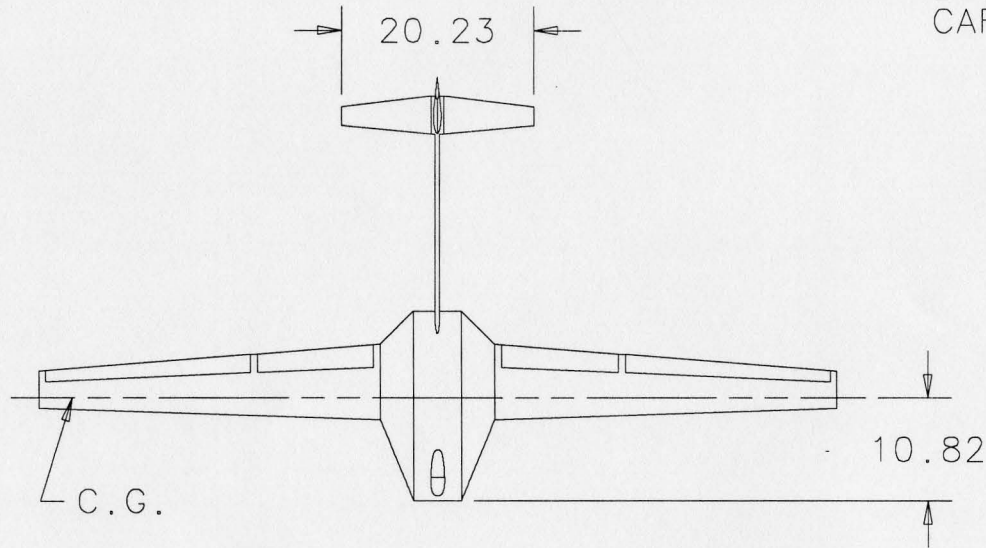
“Params” performs a fourth-order Runge-Kutta integration using the pair of first order, ordinary differential equations for velocity and distance shown above. Using the initial conditions of $V_a(0)=0$ and $x(0)=0$, these two equations were numerically integrated until the velocity equals the lift-off velocity calculated above. From this point, the rate of climb was calculated from the following equation using the lift-off velocity:

$$R / C = V_a \frac{T_a - T_R}{W}$$

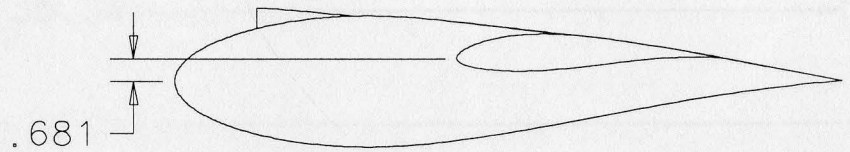
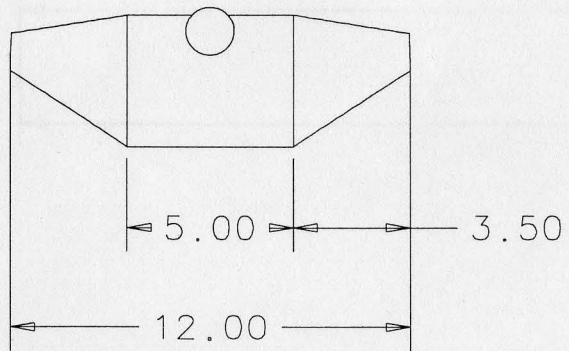
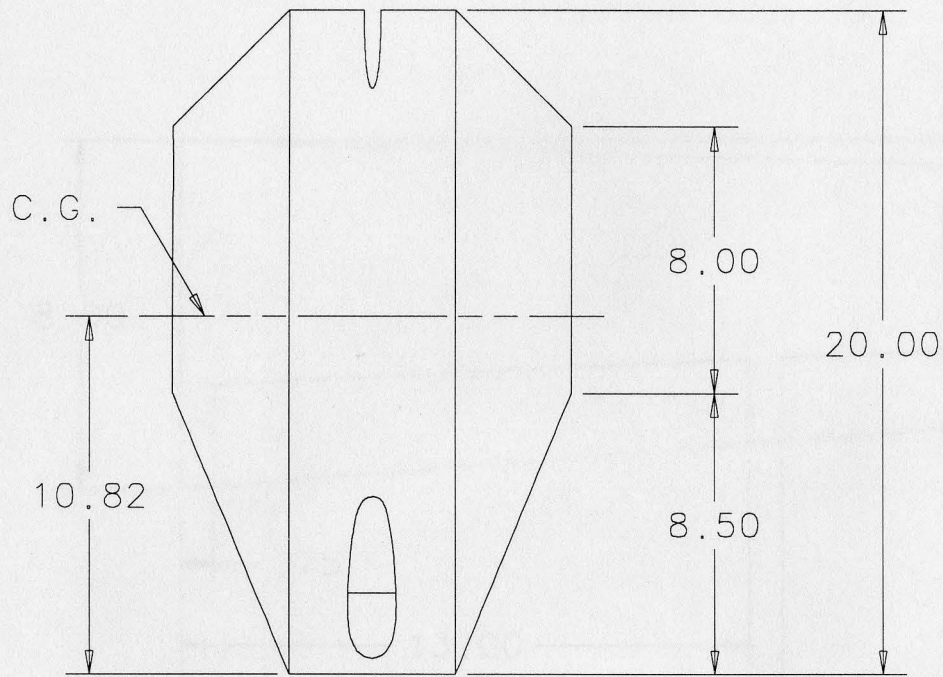
The time needed to climb six feet was calculated from the rate of climb and multiplied by the horizontal component of velocity, giving the distance needed to clear the ribbon. This distance was added to the liftoff distance calculated above to give the total distance required to takeoff and clear the six-foot ribbon.

Appendix C—Detailed Drawing Package of Final Design

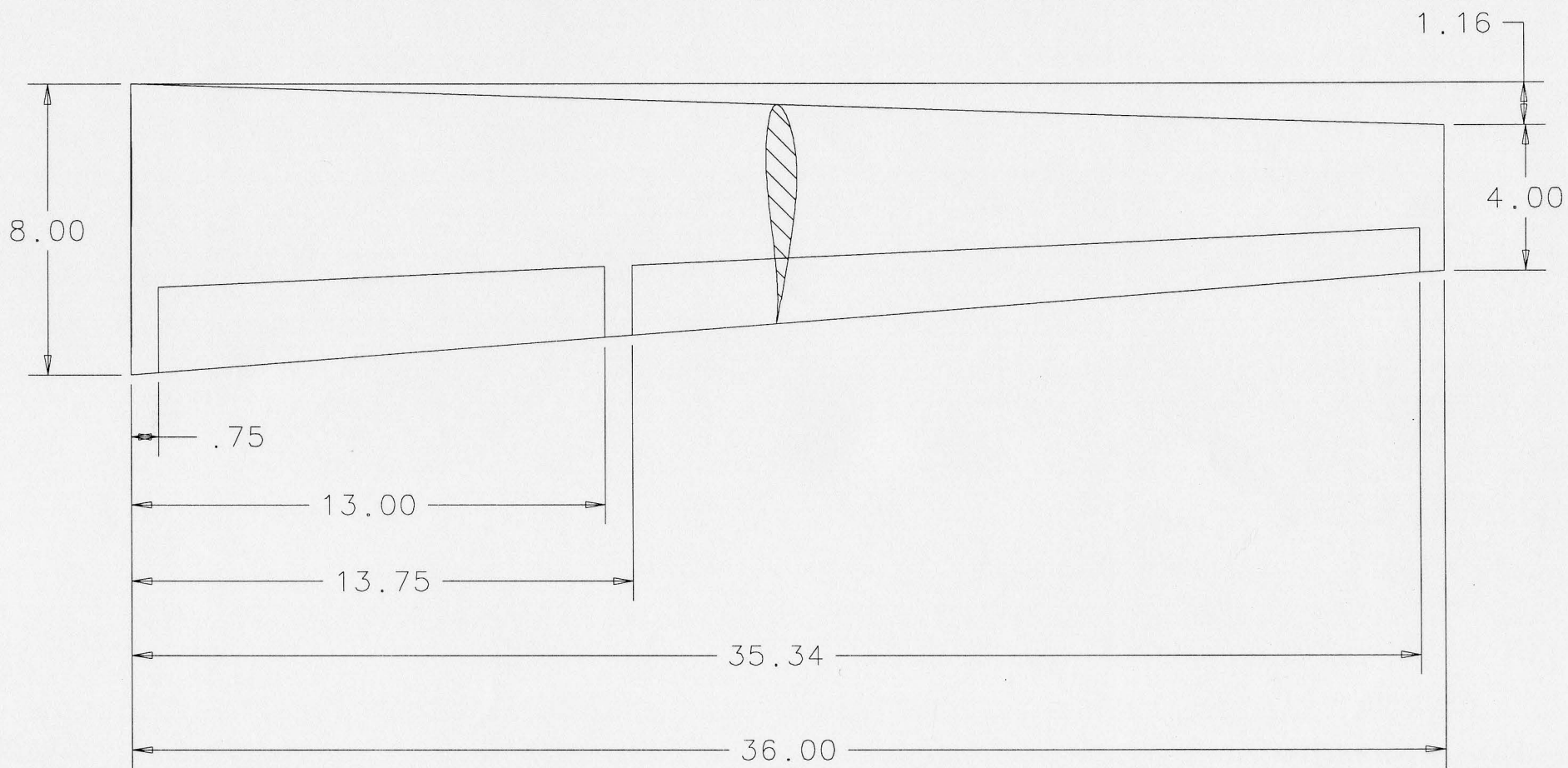
0.5050D X 0.4171D X
29.20 LEN
CARBON FIBER TUBE



ORGANIZATION		
Utah State University		
TITLE		
USU-2 AIRPLANE		
SIZE	DATE	DRAWN BY
A	02/28/98	D. Snyder
SCALE		SHEET
0.050		1 OF 6



ORGANIZATION			
Utah State University			
TITLE			
FUSELAGE			
SIZE	DATE	DRAWN BY	
A	02/28/98	D. Snyder	
SCALE		0.175	SHEET 2 OF 6



FLAP AND AILERON
WIDTH = 30% OF CHORD

ORGANIZATION

Utah State University

TITLE

Wing

SIZE

A

DATE

02/28/98

DRAWN BY

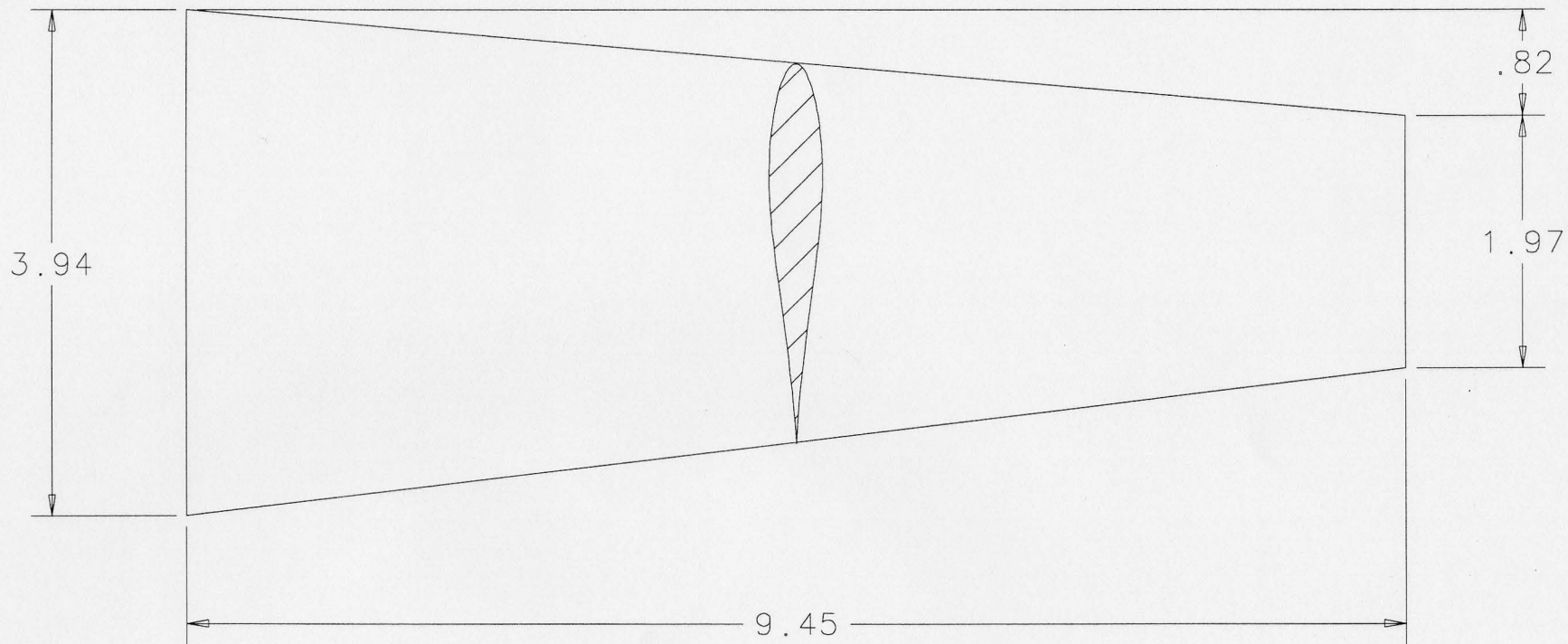
D. Snyder

SCALE

0.230

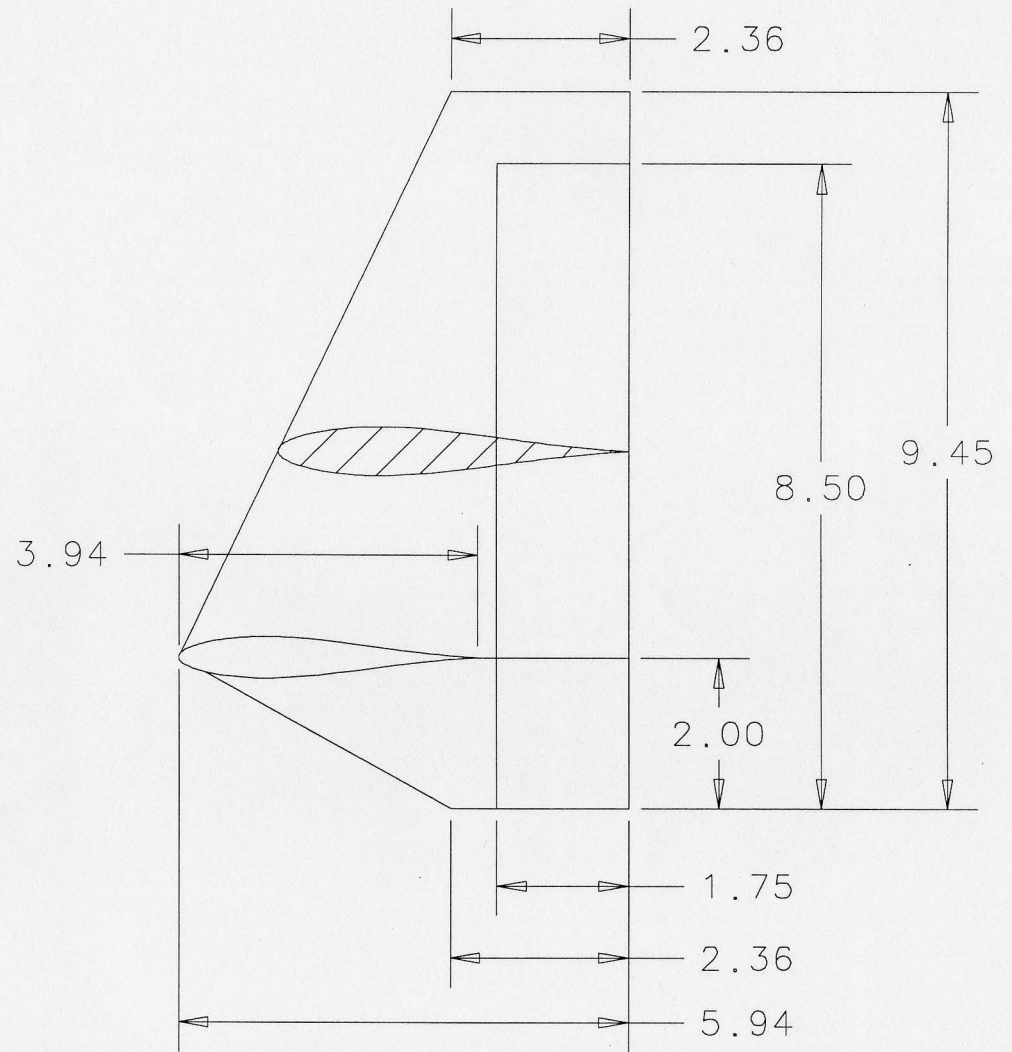
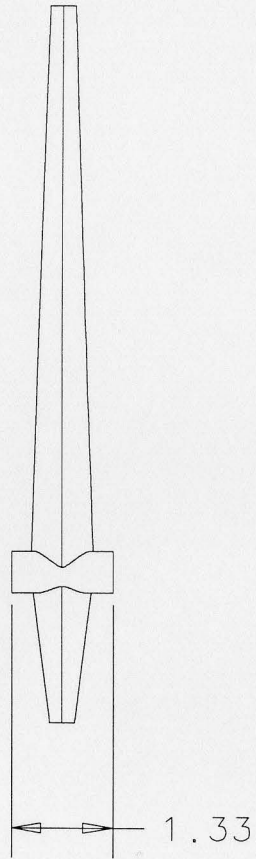
SHEET

3 OF 6

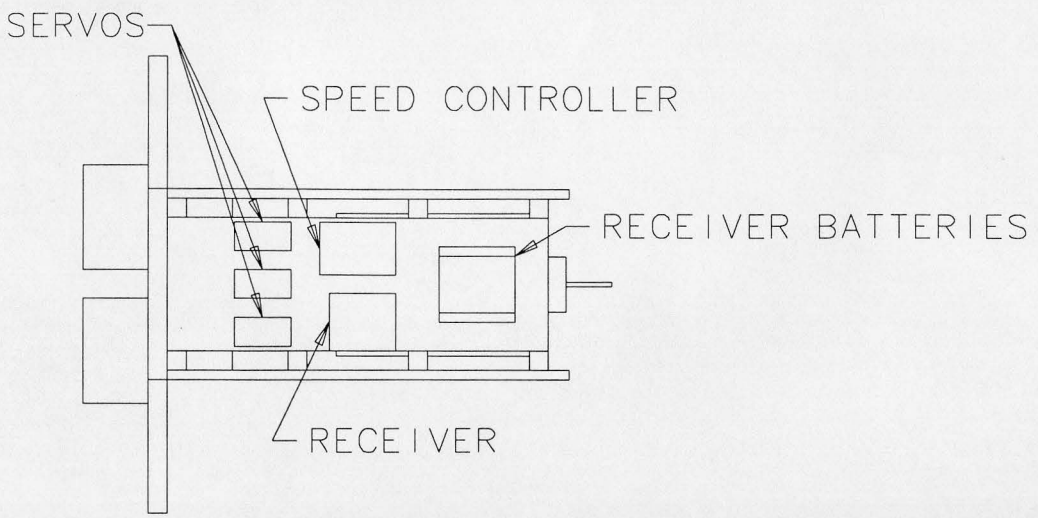
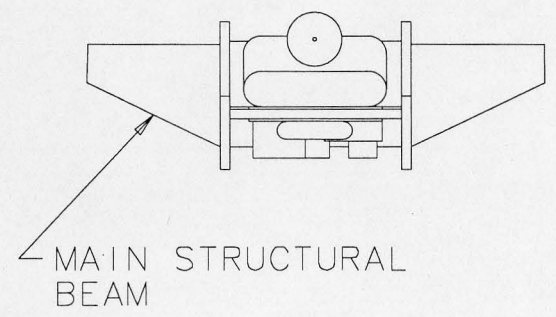
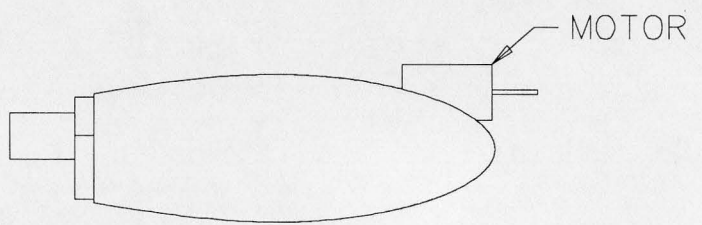
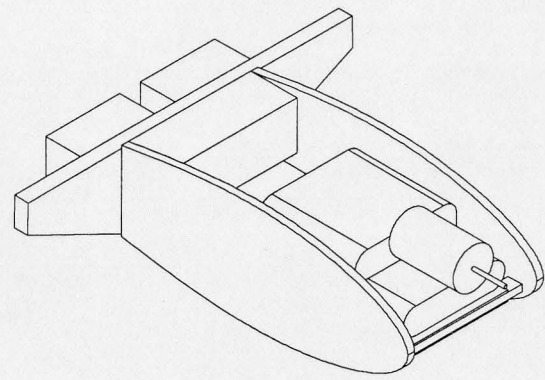
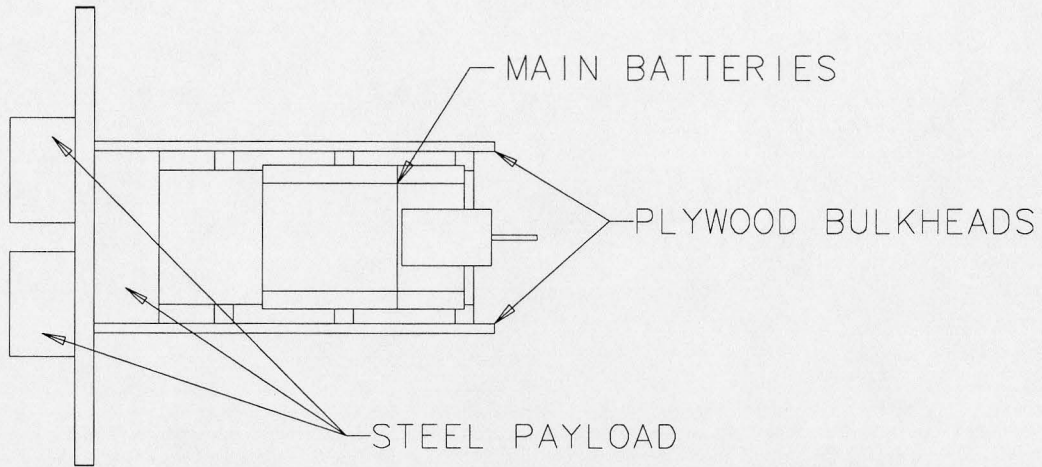


ALL-FLYING TAIL:
 ENTIRE SURFACE PIVOTS AS ELEVATOR

ORGANIZATION			
Utah State University			
TITLE			
HORIZONTAL TAIL			
SIZE	DATE	DRAWN BY	
A	02/28/98	D. Snyder	
SCALE		0.750	SHEET 4 OF 6



ORGANIZATION		
Utah State University		
TITLE		
Vertical Tail		
SIZE	DATE	DRAWN BY
A	02/28/98	D. Snyder
	SCALE	SHEET
	0.400	5 OF 6



ORGANIZATION		
Utah State University		
TITLE		
FUSELAGE INTERIOR		
SIZE	DATE	DRAWN BY
A	02/28/98	D. Snyder
SCALE		SHEET
0.200		6 OF 6